DNA ISOLATION AND MUTATION ANALYSIS. Genomic DNA was amplified using a standard polymerase chain reaction method. High-resolution melting (HRM) curve analysis (LightScanner, BioFire Defense, Salt Lake City, Utah) or denaturing high-performance liquid chromatography (dHPLC) (WAVE System Model 3500; Transgenomic, Omaha, Nebraska) were used to screen for *KCNQ1*, *KCNH2*, *SCN5A*, *KCNE1*, *KCNE2*, and *KCNJ5*. Samples in which the melting curve deviated from the wild-type control were subjected to DNA direct sequencing.

INTERPRETATION OF SEQUENCE VARIANTS. Variants of minor allele frequency (MAF) of <1% in the East Asian population from the Exome Aggregation Consortium (ExAC) were defined as rare. Combined Annotation Dependent Depletion (CADD) software was applied to predict the pathogenicity of LQTS-associated variants. CADD scores objectively integrate many diverse annotations into a single measure (C-score), and a scaled C-score of ≥10 indicates that the variant is predicted to be among the 10% most deleterious substitutions that can occur in the human genome: 1) rare and null (nonsense, frameshift, canonical with or without 1 or 2 splice sites) variants; and/or 2) rare variants with a C-score of ≥10 were considered pathogenic.

STATISTICAL ANALYSIS. The chi-square test and Fisher's exact test were used to assess the hypothesis of independence between categorical variables. The Student's *t*-test was applied for comparison of means between 2 groups. Bonferroni's correction was performed for multiple comparisons. Receiver-operator characteristic (ROC) curve analysis and the area under the ROC curve (AUC) were used to quantify the ability of Schwartz scores to detect LQTS mutation carriers. A p value of <0.05 was considered statistically significant. Statistical analysis was performed using JMP Pro 11.0.0 (SAS Institute Inc., Cary, North Carolina) and Origin 9.0 (OriginLab, Northampton, Massachusetts).

RESULTS

BASELINE CHARACTERISTICS AND ECG PARAMETERS. **Table 1** summarizes the patient characteristics for the entire cohort (n = 132) and for patients categorized according to the recovery phase QTc during exercise stress testing (QTc ≥480 ms, n = 72 vs. QTc <480 ms; n = 60). A total of 29 of 132 patients (72 women; mean age 18 ± 14 years) had a family history of LQTS, and 26 had a history of syncope or aborted cardiac arrest. More patients with a QTc ≥480 ms at the 4-min recovery phase had a positive family history or a cardiac event than those with a QTc <480 ms (**Table 1**).

Genetic analyses revealed 21 patients with 12 single *KCNQ1* mutations, 21 patients with 16 single *KCNH2* mutations, 4 patients with 4 single *SCN5A* mutations, 1 patient with a single *KCNE1* mutation, and 5 patients with 4 compound mutations (**Tables 1 and 2**). The MAFs for all mutations were <1% in the East Asian population in the ExAC data and browser, and the CADD scores for all variants were >10 (**Table 2**). Forty-four of 72 patients with prolonged QTc at the recovery phase had LQTS-related mutations, whereas 8 of 60 patients without prolonged QTc at the recovery phase had LQTS-related mutations ($p < 0.0001$). Twenty of 72 patients with a QTc ≥480 ms after exercise had LQT1 mutations, whereas there was only 1 patient of 60 patients who did not have post-exercise QTc prolongation ($p < 0.0001$) (**Table 1**).

TABLE 1 Clinical, ECG, and Genetic Characteristics of Study Patients

		Recovery Phase QTc During Exercise Stress Testing		
	Entire Cohort (n = 132)	QTc ≥480 ms (n = 72)	QTc <480 ms (n = 60)	p Value*
Age, yrs	18 ± 14	21 ± 16	14 ± 9	0.0023
Female	72 (55)	47 (65)	25 (42)	0.0068
Family history	29 (22)	24 (33)	5 (8)	0.0006
Syncope or ACA	26 (20)	20 (28)	6 (10)	0.00148
ECG at rest				
HR, beats/min	68 ± 13	66 ± 11	71 ± 14	0.0432
QTc, ms	474 ± 51	496 ± 52	447 ± 33	<0.0001
QTc ≥480 ms	50 (38)	40 (56)	10 (17)	<0.0001
Notched T-wave in 3 leads	14 (11)	12 (17)	2 (3)	0.0205
Low heart rate for age	30 (23)	14 (19)	16 (27)	0.405
Recovery phase ECG				
HR, beat/min	88 ± 20	86 ± 18	90 ± 22	0.2588
QTc, ms	490 ± 56	529 ± 44	444 ± 23	<0.0001
High probability of LQTS				
1993 criteria	32† (24)	29‡ (40)	3 (5)	<0.0001
2006 criteria	36§ (27)	31‡ (43)	5 (8)	<0.0001
2011 criteria	62 (47)	57 (79)	5 (8)	<0.0001
Mutation carriers	52 (39)	44 (61)	8 (13)	<0.0001
Mutation genes, n				
KCNQ1	21	20	1	<0.0001
KCNH2	21	15	6	0.101
SCN5A	4	4	0	0.1255
KCNE1	1	0	1	0.4545
Compound	5	5	0	0.0629

Values are mean ± SD or n (%). *p value between QTc ≥480 ms and QTc <480 ms. †p = 0.0002 versus the 2011 criteria. ‡p < 0.0001 versus the 2011 criteria. §p = 0.0014 versus the 2011 criteria.

ACA = aborted cardiac arrest; ECG = electrocardiography; HR = heart rate; LQTS = long QT syndrome.

TABLE 2 List of Mutations Found in Study Patients

Gene	Mutation	Region	MAF (ExAC, East Asian)	Score CADD	Gene	Mutation	Region	MAF (ExAC, East Asian)	Score CADD
Single mutations									
KCNQ1	S177T	S2-S3	N/A	28.8	*KCNH2*	H492Y	S2-S3	0.0001156	27
KCNQ1	D242N	S4-S5	N/A	32	*KCNH2*	R534C	S4	N/A	27.7
KCNQ1	W248F	S4-S5	N/A	28.7	*KCNH2*	G601S	S5-pore	N/A	15.53
KCNQ1	S277L	S5	N/A	32	*KCNH2*	N633I	pore	N/A	25.6
KCNQ1	Y281C	S5	N/A	25	*KCNH2*	E637K	S6	N/A	28.8
KCNQ1	A341V	S6	N/A	34	*KCNH2*	D712N	S6/CNBD	N/A	28.6
KCNQ1	IVS7+3A>G	S6	N/A	23.6	*KCNH2*	H771fsX796	S6/CNBD	N/A	35
KCNQ1	R366W	C-terminal	N/A	34	*KCNH2*	L908fsX969	C-terminal	N/A	35
KCNQ1	K422fsX431	C-terminal	N/A	35	*KCNH2*	G909fsX66	C-terminal	N/A	34
KCNQ1	R555H	C-terminal	N/A	34	*KCNH2*	G925fsX973	C-terminal	N/A	31
KCNQ1	R591H	C-terminal	N/A	32	*KCNH2*	G967fsX8	C-terminal	N/A	34
KCNQ1	IVS15+2T>C	C-terminal	N/A	14.53	*SCN5A*	A1180V	DII-DIII	0.001614	18.09
KCNH2	G53S	N-terminal	N/A	33	*SCN5A*	R1644H	DIV-S4	N/A	33
KCNH2	C64R	N-terminal	N/A	24.8	*SCN5A*	A1746T	DIV-S4	N/A	23.4
KCNH2	M124T	N-terminal	N/A	25.2	*SCN5A*	E1784K	C-terminal	N/A	33
KCNH2	P151fsX165	N-terminal	N/A	32	*KCNE1*	R98W	C-terminal	0.0001159	28.1
KCNH2	G183fsX198	N-terminal	N/A	26.4					
Compound mutations									
KCNQ1	R518X	C-terminal	N/A	39	*SCN5A*	F532C	DI-DII	0.0002703	28.2
KCNQ1	A525V	C-terminal	N/A	34	*SCN5A*	A1180V	DII-DIII	0.001614	18.09
KCNH2	P114S	N-terminal	N/A	27.3	*SCN5A*	F532C	DI-DII	0.0002703	28.2
KCNH2	P334L	N-terminal	N/A	31	*SCN5A*	D1114N	N-terminal	N/A	10.85

CADD = combined annotation dependent depletion; MAF= minor allele frequency; N/A = not available.

DISTRIBUTION OF STUDY PATIENTS ACCORDING TO EACH CRITERIA. Based on the 1993 and the 2006 LQTS criteria, 32 and 36 of 132 patients were diagnosed as having a high probability of LQTS, respectively (**Table 1**, **Figure 1**). Interestingly, the application of the 2011 criteria significantly increased the number of patients with a high probability of LQTS (32 vs. 62, 1993 vs. 2011; $p = 0.0002$, and 36 vs. 62, 2006 vs. 2011; $p = 0.0014$) (**Figure 1**). Of the 72 patients with post-exercise QTc ≥480 ms, 29 and 31 patients were diagnosed with a high probability of LQTS by the 1993 and the 2006 criteria, respectively. In contrast, 57 of these 72 patients were diagnosed with a high probability of LQTS by the 2011 criteria ($p < 0.0001$ vs. the 1993 or 2006 criteria) (**Table 1**).

FREQUENCY OF LQTS MUTATION CARRIERS AND DIAGNOSTIC PERFORMANCE FOR MUTATION CARRIERS—DIFFERENCES AMONG THE 3 DIAGNOSTIC CRITERIA. The probability of carrying mutations in patients with a high probability for LQTS was comparable among the 1993, 2006, and 2011 criteria; there were 23 of 32 patients (72%), 25 of 36 patients (69%), and 46 of 62 patients (74%), respectively (**Figure 1**). However, in the intermediate probability groups, the frequency of mutation carriers according to the 1991 and the 2006 criteria was 27 of 51 patients (53%) and 25 of 47 patients (53%), which was significantly higher than the 4 of 27 patients (15%) according to the 2011 criteria ($p < 0.0014$ vs. the 1993 criteria, and $p < 0.0013$ vs. the 2006 criteria) (**Figure 1**). **Figure 2** shows that most mutation carriers who were diagnosed with intermediate probability using the conventional criteria were diagnosed as high probability by the 2011 criteria, regardless of LQTS genotype. The application of the 2011 criteria significantly increased the number of mutation carriers with a high probability of LQTS (23 vs. 46, 1993 vs. 2011; $p < 0.0001$, and 25 vs. 46, 2006 vs. 2011; $p < 0.0001$) (**Figure 2**).

Table 3 and **Figure 3** show that a high probability of LQTS diagnosed using the 1993 and the 2006 criteria could predict mutation carriers with 44% sensitivity (23 of 52 patients) and 89% specificity (71 of 80 patients) and with 48% sensitivity (25 of 52 patients) and 86% specificity (69 of 80 patients), respectively. In contrast, a high probability diagnosed using the 2011 criteria predicted mutation carriers with 88%

FIGURE 1 Distribution of Study Patients and the Frequency of LQTS Mutation Carriers by the 1993, 2006, and 2011 Criteria

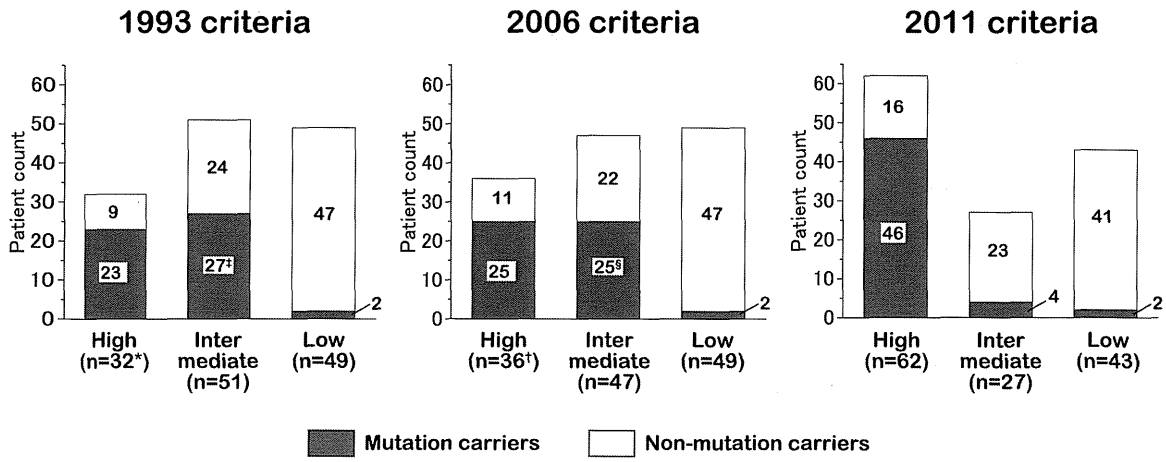

The application of the 2011 criteria significantly increased the number of patients identified with a high probability of long QT syndrome (LQTS). The probability of carrying mutations in patients with a high probability of LQTS was comparable among the 3 criteria. *p = 0.0002 or †p = 0.0014 versus high probability using the 2011 criteria; ‡p = 0.0014 or §p = 0.0013 versus mutation carriers with intermediate probability using the 2011 criteria. High = high probability of having LQTS; Intermediate = intermediate probability of having LQTS; Low = low probability of having LQTS.

sensitivity (46 of 52 patients) and 80% specificity (64 of 80 patients). The sensitivity for detecting mutation carriers was significantly different between the 1993 and the 2011 criteria, and the 2006 and the 2011 criteria ($p < 0.0001$, respectively). The negative predictive value for detecting mutation carriers with the 2011 criteria was 91%, which was significantly higher than that of the 1993 criteria (71%) or the 2006 criteria (72%) ($p = 0.001$ and $p = 0.0026$, respectively).

FIGURE 2 Classification of 52 Mutation Carriers Using the 1993, 2006, and 2011 Criteria

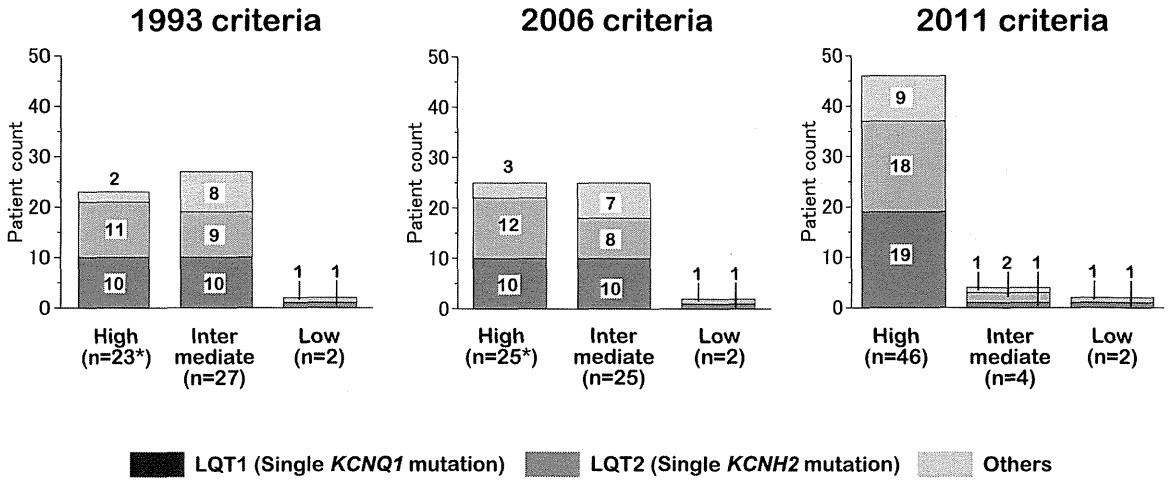

Distribution of LQTS genotype in each clinical category is also shown. *p < 0.0001 versus high probability using the 2011 criteria. Abbreviations as in **Figure 1**.

TABLE 3 Diagnostic Performance of Each Criteria and Recovery QTc for Mutation Carriers

	Genetic Analysis	
	Mutation (+)	Mutation (−)
1993 criteria		
High probability	23	9
Intermediate or low probability	29	71
2006 criteria		
High probability	25	11
Intermediate or low probability	27	69
2011 criteria		
High probability	46	16
Intermediate or low probability	6	64
QTc after exercise		
QTc ≥480 ms	44	28
QTc <480 ms	8	52

Among 52 mutation carriers, QTc ≥480 ms after exercise testing was observed in 44 patients, yielding a sensitivity of 85%. Similarly, 52 of 80 patients who were mutation-negative showed a QTc of <480 ms after exercise testing, yielding a 65% specificity (**Table 3**, **Figure 3**). The sensitivity for detecting mutation carriers using post-exercise QTc was significantly higher than that of the 1993 criteria or the 2006 criteria; however, the specificity using the post-exercise QTc was significantly lower compared with that of these criteria (**Figure 3**).

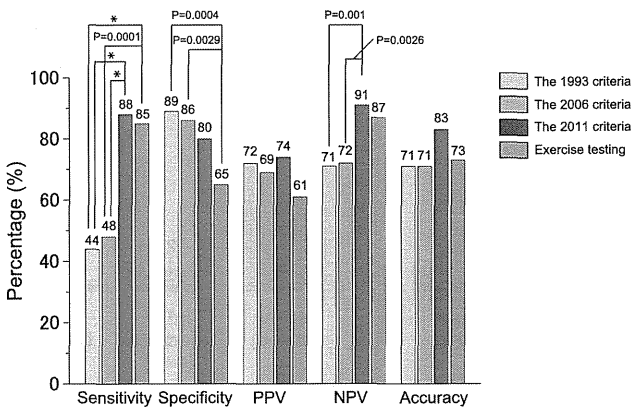

FIGURE 3 Diagnostic Performance of Each LQTS Criteria and Exercise Testing for Detection of LQTS Mutation Carriers

Sensitivity, specificity, positive predictive value (PPV), negative predictive value (NPV), and accuracy using the 1993, 2006, and 2011 criteria, and exercise testing. *p < 0.0001, between the indicated 2 groups. Abbreviation as in Figure 1.

FREQUENCY OF SYMPTOMATIC LQTS PATIENTS BY CONVENTIONAL AND UPDATED CRITERIA. In our cohort, 26 patients were symptomatic (syncope in 25 patients and aborted cardiac arrest in 1 patient) before the introduction of beta-blocker therapy (**Table 1**, **Figure 4**). The frequency of symptomatic patients in those with a high probability using the 1993 criteria was 59% (19 of 32 patients), which was higher compared with the 34% (21 of 62 patients) using the 2011 criteria ($p = 0.0272$). However, the difference was not significant after the Bonferroni correction (**Figure 4**).

DIAGNOSTIC PERFORMANCE OF THE UPDATED CRITERIA. To confirm the diagnostic accuracy of the 2011 updated criteria, ROC curves were constructed for predicting LQTS mutation carriers and detecting symptomatic LQTS patients using the updated criteria. The AUC for LQTS mutation carriers was 0.88 (95% confidence interval: 0.81 to 0.94) (**Figure 5**). The optimal cutoff value for predicting LQTS mutation carriers was 3.5.

DISCUSSION

The present study demonstrated that 1) more patients were diagnosed with a high probability of LQTS by the 2011 criteria compared with the 1993 or the 2006 criteria (**Figure 1**); 2) in the groups with intermediate probability of LQTS, more mutation carriers were diagnosed in the 1993 or the 2006 than in the 2011 criteria group (**Figure 1**); and 3) both the sensitivity and the negative predictive value for detecting mutation carriers using the 2011 criteria were significantly higher than those of the 1993 or the 2011 criteria (**Figures 1 and 3**, **Table 3**).

Schwartz et al. proposed a first set of diagnostic criteria for LQTS in 1985, which provided a logical and quantitative approach to the clinical diagnosis of LQTS (6). They reported LQTS diagnostic criteria in 1993 based on clinical presentation, including ECG, and clinical and familial findings (7), and arbitrarily modified the criteria in 2006 (12). Recently, the diagnostic criteria were updated by adding a more objective parameter, the evaluation of the recovery phase of exercise (18). Vincent et al. (13) reported that the QTc of normal subjects showed no significant changes during exercise compared with the value at rest, whereas those with Romano-Ward syndrome demonstrated a significant increase in QTc both before and after exercise. In this study, 29 of 32 patients, 31 of 36 patients, and 57 of 62 with a high probability of LQTS diagnosed by the 1993, the 2006, or the 2011

criteria, respectively, showed prolonged QTc ≥480 ms after exercise (**Table 1**).

Asymptomatic mutation carriers who show a normal QT interval might be overlooked by applying the 1993 LQTS diagnostic criteria, because these criteria do not consider any molecular diagnostic characteristics of LQTS. A previous study showed a correlation between the conventional Schwartz score and the results of genetic testing (10). In 123 patients with a high probability of LQTS (score ≥4), 89 patients were genotype-positive (72%), whereas among 215 patients with a score <4, 93 patients were still genotype-positive (43%) (10). In addition, in this study, the percentages of positive genotypes in patients with high and intermediate probability by the 1993 criteria were 72% and 53%, respectively. These percentages were comparable with those calculated using the 2006 criteria (69% and 53%). In contrast, the application of the 2011 criteria resulted in the maintenance of the percentage of genotype-positive patients with a high probability of LQTS (74%), while significantly reducing that in patients with intermediate probability (15%; p = 0.0002 vs. the 1993 criteria, and p = 0.0014 vs. the 2006 criteria), regardless of the LQTS genotype (**Figure 2**).

The 1993 LQTS diagnostic criteria also had low sensitivity in identifying disease carriers. A previous study showed that 89 of 218 genotype-positive LQTS patients were diagnosed with a high probability of LQTS, yielding a 41% sensitivity (10). This value was similar to our results: 44% by the 1993 criteria and 48% by the 2006 criteria. In contrast, the sensitivity significantly increased to 88% using the 2011 criteria. In this way, the 2011 criteria could detect more asymptomatic LQTS mutation carriers in addition to symptomatic LQTS patients in advance of gene analysis.

Several studies reported that further QTc prolongation after exercise could be useful for identifying LQTS mutation carriers (14,15). Horner et al. (15) performed treadmill stress tests in 243 LQTS patients and showed that stress testing could unmask patients with occult LQTS, particularly LQT1. They also reported that LQT2 and LQT3 patients responded similarly to each other in peak exercise with an initial shortening of their QTc, which was then followed by a gradual increase in their QTc in recovery, which approached their respective QTc intervals at rest (15). In this study, the prolonged QTc ≥480 ms after exercise predicted mutation carriers with 85% sensitivity and 65% specificity. The sensitivity of this test is reasonable; however, the specificity was lower compared with that of the 1993 or the 2006 diagnostic criteria.

FIGURE 4 The Frequency of Symptomatic LQTS Patients Before Therapy According to the 1993, 2006, and 2011 Criteria

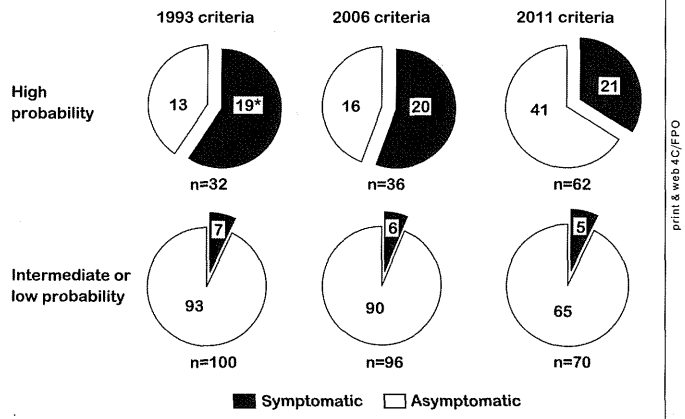

The frequency of symptomatic patients with a high probability of LQTS according to the 1993 criteria was significantly higher than that according to the 2006 criteria and the 2011 criteria. *p = 0.0272 versus the frequency of symptomatic LQTS patients by the 2011 criteria.

The number of symptomatic LQTS patients in the group with a high probability of LQTS were similar, irrespective of the diagnostic criteria used (19 using the 1993 criteria and 20 using the 2006 criteria vs. 21 using the 2011 criteria) (**Figure 4**). However, the proportion of symptomatic patients with a higher

FIGURE 5 Diagnostic Performance of the Updated Criteria

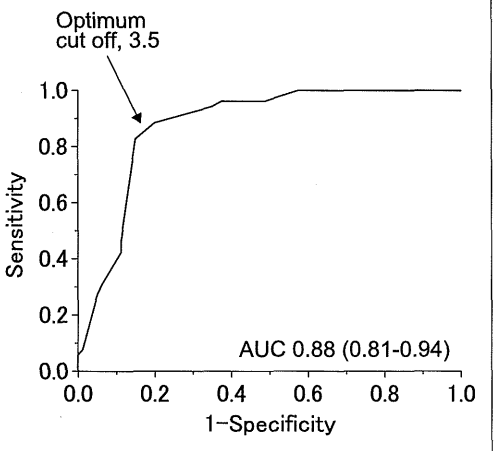

Receiver-operator characteristic (ROC) curve analysis with corresponding area under the curves (AUCs) displaying the diagnostic performance of updated criteria for the detection of LQTS mutation carriers. Abbreviation as in Figure 1.

probability of LQTS diagnosed using the 1993 criteria (59%) was higher compared with that of patients diagnosed using the 2011 criteria (34%). Based on these findings, the 1993 criteria could be useful for detecting more symptomatic LQTS patients.

STUDY LIMITATIONS. First, it was a retrospective study with a modest sample size. However, this study demonstrated the significance of the 2011 criteria in terms of an increase in the diagnosis of patients with a high probability of LQTS-related gene mutations. Statistical significance with small sample sizes might be spurious, and conclusions might be limited. In addition, some statistical comparisons were made between subsamples, which might further limit confidence in the results, especially whether they were statistically significant. Second, genetic screening were performed by HRM or dHPLC followed by Sanger sequencing. However, these techniques have been used successfully for screening. Compared with DNA sequencing, the overall sensitivity and specificity of HRM were 0.99 and 0.96, and those of dHLPC were 0.88 and 0.97, respectively (21). Finally, the genotyped mutation carriers in this study were mainly LQT1 and LQT2 genotyped patients. However, because the most prevalent forms of LQTS are LQT1 and LQT2 in general, our study population did not limit the generalizability of results.

CONCLUSIONS

These results demonstrate that the 2011 LQTS diagnostic criteria can identify more silent LQTS-related gene mutation carriers as being at a high probability of LQTS, which cannot be identified by the conventional criteria. We suggest that the use of the 2011 criteria will facilitate the diagnosis of LQTS and will avoid a number of false negative results.

ACKNOWLEDGMENTS The authors gratefully acknowledge Akihiro Nomura for helpful discussions, and Takako Obayashi, Masako Fukagawa, Hitomi Oikawa, Kazu Toyo-oka, Madoka Tanimoto, and Arisa Ikeda for technical assistance.

REPRINT REQUESTS AND CORRESPONDENCE: Dr. Masakazu Yamagishi, Division of Cardiovascular Medicine, Kanazawa University Graduate School of Medicine, 13-1, Takara-machi, Kanazawa, Ishikawa 920-8640, Japan. E-mail: myamagi@med.kanazawa-u.ac.jp.

PERSPECTIVES

COMPETENCY IN MEDICAL KNOWLEDGE: LQTS is diagnosed in the presence of an LQTS risk score of ≥3.5 and/or an unequivocally pathogenic mutation in 1 of the LQTS genes, or a QTc of ≥500 ms in repeated 12-lead ECG. Asymptomatic mutation carriers with a normal QT interval might be overlooked by applying the conventional LQTS diagnostic criteria.

TRANSLATIONAL OUTLOOK: The 2011 LQTS diagnostic criteria can identify more silent LQTS-related gene mutation carriers as having a high probability of LQTS, which cannot be identified by the conventional criteria. Further larger studies with a comprehensive mutation analysis are required to establish the utility of the 2011 criteria for clinical detection of LQTS patients with gene mutations.

REFERENCES

1. Moss AJ, Schwartz PJ, Crampton RS, et al. The long QT syndrome. Prospective longitudinal study of 328 families. Circulation 1991;84:1136-44.

2. Kawashiri MA, Hayashi K, Konno T, Fujino N, Ino H, Yamagishi M. Current perspectives in genetic cardiovascular disorders: from basic to clinical aspects. Heart Vessels 2014;29:129-41.

3. Hayashi K, Shimizu M, Ino H, et al. Characterization of a novel missense mutation E637K in the pore-S6 loop of HERG in a patient with long QT syndrome. Cardiovasc Res 2002;54:67-76.

4. Hayashi K, Fujino N, Uchiyama K, et al. Long QT syndrome and associated gene mutation carriers in Japanese children: results from ECG screening examinations. Clin Sci (Lond) 2009;117:415-24.

5. Schwartz PJ, Ackerman MJ, George AL, Jr., Wilde AA. Impact of genetics on the clinical management of channelopathies. J Am Coll Cardiol 2013;62:169-80.

6. Schwartz PJ. Idiopathic long QT syndrome: progress and questions. Am Heart J 1985;109:399-411.

7. Schwartz PJ, Moss AJ, Vincent GM, Crampton RS. Diagnostic criteria for the long QT syndrome. An update. Circulation 1993;88:782-4.

8. Priori SG, Napolitano C, Schwartz PJ. Low penetrance in the long-QT syndrome: clinical impact. Circulation 1999;99:529-33.

9. Priori SG, Schwartz PJ, Napolitano C, et al. Risk stratification in the long-QT syndrome. N Engl J Med 2003;348:1866-74.

10. Tester DJ, Will ML, Haglund CM, Ackerman MJ. Effect of clinical phenotype on yield of long QT syndrome genetic testing. J Am Coll Cardiol 2006;47:764-8.

11. Roden DM. Drug-induced prolongation of the QT interval. N Engl J Med 2004;350:1013-22.

12. Schwartz PJ. The congenital long QT syndromes from genotype to phenotype: clinical implications. J Intern Med 2006;259:39-47.

13. Vincent GM, Jaiswal D, Timothy KW. Effects of exercise on heart rate, QT, QTc and QT/QS2 in the Romano-Ward inherited long QT syndrome. Am J Cardiol 1991;68:498-503.

14. Takenaka K, Ai T, Shimizu W, et al. Exercise stress test amplifies genotype-phenotype correlation in the LQT1 and LQT2 forms of the long-QT syndrome. Circulation 2003;107:838-44.

15. Horner JM, Horner MM, Ackerman MJ. The diagnostic utility of recovery phase QTc during

treadmill exercise stress testing in the evaluation of long QT syndrome. Heart Rhythm 2011;8: 1698-704.

16. Ackerman MJ, Khositseth A, Tester DJ, Hejlik JB, Shen WK, Porter CB. Epinephrine-induced QT interval prolongation: a gene-specific paradoxical response in congenital long QT syndrome. Mayo Clin Proc 2002;77:413-21.

17. Shimizu W, Noda T, Takaki H, et al. Epinephrine unmasks latent mutation carriers with LQT1 form of congenital long-QT syndrome. J Am Coll Cardiol 2003;41:633-42.

18. Schwartz PJ, Crotti L. QTc behavior during exercise and genetic testing for the long-QT syndrome. Circulation 2011;124:2181-4.

19. Priori SG, Wilde AA, Horie M, et al. HRS/EHRA/APHRS expert consensus statement on the diagnosis and management of patients with inherited primary arrhythmia syndromes: document endorsed by HRS, EHRA, and APHRS in May 2013 and by ACCF, AHA, PACES, and AEPC in June 2013. Heart Rhythm 2013;10:1932-63.

20. Tester DJ SP, Ackerman MJ. Congenital long QT syndrome. In: Gussak I, Antzelevitch C, eds. Electorical diseases of the heart. 2nd Ed. Berlin, Germany: Springer, 2013: 439-68.

21. Liu YP, Wu HY, Yang X, et al. Diagnostic accuracy of high resolution melting analysis for detection of KRAS mutations: a systematic review and meta-analysis. Scientific Reports 2014;4:7521.

KEY WORDS diagnosis, diagnostic method, genetics, long QT syndrome

Impact of Updated Diagnostic Criteria for Long QT Syndrome on Clinical Detection of Diseased Patients: Results From a Study of Patients Carrying Gene Mutations

Kenshi Hayashi, Tetsuo Konno, Noboru Fujino, Hideki Itoh, Yusuke Fujii, Yoko Imi-Hashida, Hayato Tada, Toyonobu Tsuda, Yoshihiro Tanaka, Takekatsu Saito, Hidekazu Ino, Masa-aki Kawashiri, Kunio Ohta, Minoru Horie, Masakazu Yamagishi

Hayashi et al. scored patients with the long QT syndrome (LQTS) using Schwartz diagnostic criteria, and examined the validation of the criteria relevant to the frequency of LQTS-related gene mutation. This study showed more patients were diagnosed with a high probability of LQTS by the 2011 criteria compared with the conventional criteria. Both the sensitivity and the negative predictive value using the 2011 criteria for detecting mutation carriers were significantly higher than that of the conventional criteria. The proportion of symptomatic patients with a high probability of LQTS diagnosed using the 1993 criteria was higher than that of patients diagnosed using the 2011 criteria.

oooo

ARTICLE IN PRESS

Journal of Arrhythmia ■ (■■■■) ■■■–■■■

Contents lists available at ScienceDirect

Journal of Arrhythmia

journal homepage: www.elsevier.com/locate/joa

Review

Inherited bradyarrhythmia: A diverse genetic background

Taisuke Ishikawa, DVM, PhD, Yukiomi Tsuji, MD, PhD, Naomasa Makita, MD, PhD*

Department of Molecular Physiology, Nagasaki University Graduate School of Biomedical Sciences, 1-12-4 Sakamoto, Nagasaki 852-8523, Japan

ARTICLE INFO

Article history:
Received 11 August 2015
Received in revised form
3 September 2015
Accepted 16 September 2015

Keywords:
Bradyarrhythmia
Genome-wide association studies
Ion channel
Sinus node
Cardiac conduction system

ABSTRACT

Bradyarrhythmia is a common heart rhythm abnormality comprising number of diseases and is associated with decreased heart rate due to the failure of action potential generation and propagation at the sinus node. Permanent pacemaker implantation is often used therapeutically to compensate for decreased heart rate and cardiac output. The vast majority of bradyarrhythmia cases are attributable either to aging or to structural abnormalities of the cardiac conduction system, caused by underlying structural heart disease. However, there is a subset of bradyarrhythmia primarily caused by genetic defects in the absence of aging or underlying structural heart disease. These include several genes that play principal roles in cardiac electrophysiology, heart development, cardioprotection, and the structural integrity of the membrane and sarcomere. Recent advances in the functional analysis of mutations using a heterologous expression system and genetically engineered animal models have provided significant insights into the underlying molecular mechanisms responsible for inherited arrhythmia. In this review, current understandings of the genetic and molecular basis of inherited bradyarrhythmia are presented.

Contents

* Corresponding author. Tel.: +81 95 819 7031; fax: +81 95 819 7911.
E-mail address: makitan@nagasaki-u.ac.jp (N. Makita).

http://dx.doi.org/10.1016/j.joa.2015.09.009
1880-4276/

Please cite this article as: Ishikawa T, et al. Inherited bradyarrhythmia: A diverse genetic background. J Arrhythmia (2015), http://dx.doi.org/10.1016/j.joa.2015.09.009i

1. Introduction

Bradyarrhythmia is a serious electrical disorder of the heart with the potential to be life threating. The condition is caused by an electrical dissociation in the cardiac conduction system (CCS) comprising the sinus bradycardia, the sinoatrial (SA) exit block and the atrioventricular block (AVB). It often manifests as abnormally suppressed cardiac output in affected individuals, requiring permanent pacemaker implantation in order to compensate for decreased heart rate. The CCS is equipped with a sophisticated histological structure and specialized cellular function in order to maintain proper impulse generation and propagation. The mechanical burden and scars resulting from structural heart disease are a major cause of bradyarrhythmia. Accumulation of connective tissue such as collagen is almost always associated with progression of heart failure, as it promotes dissociation between electrically coupled cardiomyocytes [1]. Collagen deposition is associated with aging and underlying structural heart disease, reflected by the increased incidence and prevalence of bradyarrhythmia associated with these factors [1,2]. In the absence of underlying structural disease or aging, bradyarrhythmia may occur primarily due to genetic defects. In this review, we aim to describe the current understanding of inherited bradyarrhythmia with a focus on diverse genetic backgrounds and molecular physiology (Fig. 1 and Table 1).

2. Modulation mechanisms of heart rate and genetic exacerbation factors: physiological regulation of sinus rhythm

In the CCS, the sinoatrial node (SAN) is the primary pacemaker component and functions as a resource for automaticity; that is, spontaneous depolarization with regular intervals. Histologically, the SAN is intramurally embedded at the junction of the right atrium and the superior vena cava and lies along the crista terminalis [3]. The SAN displays heterogeneous cellular morphology, action potential configuration, and electrophysiological characteristics [4]. The SAN's major pacemaker site is situated at its center, however; this site may shift peripherally depending on various interventional factors such as electrolyte concentrations, autonomic nervous stimuli, and temperature [3]. The underlying mechanisms of this pacemaker shift remain undetermined, however; the pacemaker tends to shift to the site where electrical activity is least suppressed by extrinsic factors [3]. The molecular mechanisms underlying myocyte firing in the central SAN are characterized by the SAN's unique gene expression profile, with minimal expression of *KCNJ2* (inwardly rectifying K channel, Kir2.1) and *SCN5A* (cardiac Na channel, Nav1.5) and higher expression of *HCN4* (the pacemaker channel). The absence of *KCNJ2* expression allows the resting membrane potential depolarized to enable spontaneous depolarization, while the absence of *SCN5A* expression can prevent rapid upstroke of action potential. Abundant expression of the *HCN4* pacemaker channel promotes spontaneous, slow depolarization in response to phase 4 hyperpolarization. The peripheral SAN, on the other hand, partially shares the gene expression profile and electrophysiological characteristics of the atrial myocytes [3]. The major role of excitation in the peripheral SAN is the rapid transmission of the sinus impulse to surrounding atrial myocytes. An abundant expression of *SCN5A* causes fast upstroke of action potential in phase 0 and this gives rise to rapid electrical conduction in the peripheral SAN. Thus, loss-of-function mutations in *SCN5A* could result in SA exit block, an electrical conduction blockade between the central SAN and surrounding atrial myocytes [5].

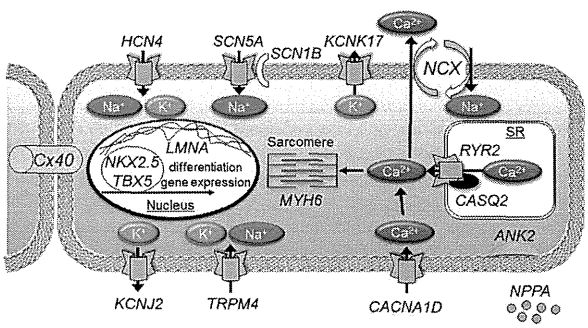

Fig. 1. Molecular modules involved in inherited bradyarrhythmia. Abnormalities in multiple pathways involving membrane ion channels, SR ion channels, sarcomere components, cardiac hormones, and membrane anchor proteins are associated with inherited bradyarrhythmia.

The mechanism of cyclic activation in voltage-gated ion channels involves the action of the pacemaker current on the cell membrane and is known as a membrane clock. Recently, a growing body of evidence has implicated the involvement of additional complementary mechanisms in this process, in particular, the rhythmic spontaneous release of Ca^{2+} by the sarcoplasmic reticulum (SR), which is referred to as a calcium clock. The calcium clock functions collaboratively with the membrane clock to form a unified, automatic system, known as a coupled-clock pacemaker system [6]. Genetic defects in the genes involved in membrane and calcium clocks can potentially cause SA disorders.

2.1. HCN4

In mammals, the hyperpolarized-activated cyclic nucleotide-gated channel (HCN) family is comprised of four distinct genes, *HCN1, 2, 3* and *4*; that are expressed in a wide variety of excitable cells (*HCN4* is predominantly expressed in the central SAN) [7]. *HCN4* slowly becomes permeable for K^+ and Na^+ in response to hyperpolarization, thus giving rise to slow diastolic depolarization resulting in automaticity [7]. Since the first description of an *HCN4* mutation in familial sick sinus syndrome (SSS) [8], twenty-two further mutations have been reported. Patch-clamp analysis of these mutations using a heterologous expression system with *Xenopus oocytes* or cultured cell lines have shown that reduced peak current densities or a hyperpolarizing shift of the voltage-dependence of activation are the major causes of disease [9,10]. Indeed, these loss-of-function properties decrease the slope of diastolic depolarization, resulting in sinus bradycardia. Some *HCN4* mutations disrupt the cyclic-nucleotide binding domain (cNBD) to which cyclic nucleotide cAMP and cGMP bind directly in response to β-adrenergic stimuli [8,9,11]. However, the molecular mechanisms of *HCN4* mutations are not yet fully elucidated; for example, G482R has been reported in multiple families associated with sinus bradycardia and left ventricular noncompaction cardiomyopathy [7,12]; however, the molecular mechanism underlying left ventricular noncompaction remains unknown.

2.2. SCN5A

The cardiac Na channel α subunit Nav1.5 encoded by *SCN5A* is associated with auxiliary β-subunits Navβ1 and Navβ3 [13]. Activation of the sodium channel initiates a rapid influx of Na^+, giving rise to the phase 0 upstroke of cardiac action potential, which in turn triggers depolarization of neighboring cardiomyocytes [13]. As this Na^+ influx determines the slope and amplitude of phase 0, mutations in *SCN5A* may affect cardiac conduction velocity. The genetic defects in *SCN5A* are associated with multiple diverse inherited arrhythmias referred to as cardiac sodium channelopathy and include type-3 long QT

Please cite this article as: Ishikawa T, et al. Inherited bradyarrhythmia: A diverse genetic background. J Arrhythmia (2015), http://dx.doi.org/10.1016/j.joa.2015.09.009i

Table 1
Genes responsible for inherited bradyarrhythmia.

Gene name	Protein name	Inheritance mode	Atrial phenotypes	Conduction diseases	Ventricle phenotypes	Additional phenotypes	Function
Ion channels							
HCN4	HCN4	AD	Sinus bradycardia		LVNC, BrS		Loss
SCN5A	Nav1.5	AD, AR	Sinoatrial block, AF, Atrial standstill	PCCD, AVB	LQT3, BrS, DCM		Loss
SCN10A	Nav1.8	AD?	AF?	?	BrS?	Association with conduction parameters in ECG, episodic pain syndrome	?
SCN1B	Navβ1	AD		BBB	BrS	Epilepsy	Loss
KCNJ2	Kir2.1	AD			LQT7(ATS), SQT, BrS	Periodic paralysis, dysmorphic features	
CACNA1D	Cav1.3	AD	Sinus bradycardia			Congenital deafness	Loss
KCNK17	TASK-4	AD		PCCD, AVB, BBB	IVF?		Gain
TRPM4	TRPM4	AD		PCCD, AVB, BBB	BrS		Gain
Ca^{2+} handling proteins on the sarcoplasmic reticulum							
RYR2	Ryanodine receptor 2	AD	Sinus bradycardia		CPVT, ARVC		Loss
CASQ2	Calsequestrin	AR	Sinus bradycardia		CPVT		Loss
Gap junction channel							
GJA5	Connexin40	AD		PCCD, AVB, BBB			Loss
Cardiac hormone							
NPPA	ANP	AD	Atrial standstill, Biatrial dilatation				Loss
Transcription factors							
TBX5	Tbx5	AD	ASD, AF	AVB	VSD	Hand anomalies (heart-hand syndrome)	Loss/gain
Nuclear membrane component							
LMNA	Lamin A/C	AD		PCCD, AVB	DCM	Laminopathies including muscular dystrophy and Hutchinson–Gilford progeria syndrome	Loss
Membrane adaptor protein							
ANK2	Ankyrin-B	AD	Sinus bradycardia	PCCD	LQT4		Loss
Sarcomere protein							
MYH6	Atrial myosin heavy chain	AD	Sinus bradycardia, AF, ASD		HCM, DCM		Loss

AD, autosomal dominant; AR, autosomal recessive; LQT, long QT; AVB, atrioventricular block; BrS, Brugada syndrome; BBB, bundle branch block; LVNC, left ventricular noncompaction; CPVT, catecholaminergic ventricular tachycardia; ATS, Andersen–Tawil syndrome; ASD, atrial septal defect; VSD, ventricular septal defect; PCCD, progressive cardiac conduction defect; AF, atrial fibrillation; HCM, hypertrophic cardiomyopathy; DCM, dilated cardiomyopathy; IVF, idiopathic ventricular fibrillation.

syndrome, Brugada syndrome, SSS, atrial fibrillation (AF), progressive cardiac conduction defect (PCCD), dilated cardiomyopathy (DCM) and sudden infant death syndrome [13]. Patients with *SCN5A* mutations often display mixed arrhythmic phenotypes of cardiac sodium channelopathy, known as overlap syndrome [14]. As mentioned above, the molecular basis for SSS resulting from *SCN5A* mutations is an exit block at the peripheral SAN, caused by decreased conduction velocity from the central SAN [5]. Likewise, impaired sodium channel function may cause a conduction block within the CCS, referred to as AVB or bundle branch block (BBB). The presence of *SCN5A* mutations may distinctly affect the clinical outcomes associated with several arrhythmias. In Brugada syndrome, *SCN5A* mutations are associated with prolonged interatrial conduction times and AF induction; however, they do not appear to be related to spontaneous AF episodes, among other clinical variables [15]. In SSS, *SCN5A* mutation carriers exhibit significantly early onset as well as profound male predominance, thus resembling Brugada syndrome with a considerably earlier age of onset [16].

2.3. Mutations in genes responsible for calcium regulation

The third gene responsible for SSS is *ANK2*, which encodes the anchor protein ankyrin-B, thus linking integral membrane proteins to the underlying spectrin–actin cytoskeleton of cardiomyocytes [17]. Genetically engineered *Ank2* heterozygote knockout mice develop sinus bradycardia and exercise-induced aberrant ventricular tachycardia due to a Ca^{2+}-handling abnormality [18]. Immunohistochemical analysis of cardiomyocytes from these mice showed mislocalization of the Na^+/Ca^{2+} exchanger, Na^+/K^+-ATPase, and the IP3 receptor [19,20]. Biophysical analysis of SAN cells using a patch-clamp identified reduced currents in the Na^+/Ca^{2+} exchanger and L-type Ca^{2+} channels [17]. These observations suggest that human *ANK2* mutations may predispose individuals to SAN dysfunction as a result of the biophysical disturbance of multiple proteins involved in Ca^{2+}-handling.

The Cav voltage-gated Ca^{2+} channels, Cav1.2 and Cav1.3, mediate L-type Ca^{2+} current essential for normal cardiac pacemaker activity and conduction in both the SAN and the atrioventricular node. Cav1.3 activates more rapidly and under more

Please cite this article as: Ishikawa T, et al. Inherited bradyarrhythmia: A diverse genetic background. J Arrhythmia (2015), http://dx.doi.org/10.1016/j.joa.2015.09.009i

hyperpolarized membrane potentials when compared with Cav1.2 [21]. These properties allow Cav1.3 to contribute more significantly to the diastolic depolarization of SAN cells. Loss-of-function mutations in the *CACNA1D* encoding Cav1.3 cause SAN dysfunction with congenital deafness, attributable to the loss of rapid activation kinetics and negative activation thresholds of Cav1.3 in humans [22], which is consistent with the phenotypes observed in mice with genetic inactivation of *CACNA1D* [23].

Genes responsible for sinus bradycardia via abnormal Ca^{2+} regulation include the ryanodine receptor *RYR2* and the calsequestrin *CASQ2*, both of which are known to be causative genes for catecholaminergic polymorphic ventricular tachycardia (CPVT) [24–26]. CPVT-related mutations in these genes affect Ca^{2+} regulation by disrupting its storage and release from the SR during periods of exercise or emotional stress, resulting in sinus bradycardia and fatal ventricular tachyarrhythmia [27]. Postma et al. found a markedly lower resting heart rate in CPVT probands and their family members with *RYR2* mutations when compared with those of non-carrier family members [25]. They further reported that CPVT patients with *CASQ2* mutations develop sinus bradycardia, consistent with observations in *Casq2* homozygote knockout mice [24]. The identification of gene mutations contributing to Ca^{2+} release and storage in the SR served to reinforce the critical role of calcium clocks in the maintenance of normal sinus rhythm.

3. Genetic basis for atrial standstill

3.1. SCN5A

SCN5A is abundantly expressed throughout the ventricular working myocardium and the CCS, as well as in the atrium [13]. Certain *SCN5A* mutations cause conduction block in the entire atrium, leading to atrial standstill and SSS [16,28]. A retrospective study of patients who experienced cardiac device-lead capture issues, including atrial standstill, showed a high prevalence of loss-of-function *SCN5A* mutations [29].

3.2. NPPA

Mutations in *NPPA*, the gene encoding atrial natriuretic peptide (ANP), are associated with certain atrial arrhythmias [30,31]. A deletion mutation in *NPPA* has been identified in an AF family spanning three generations. Affected members exhibited a transition from paroxysmal to chronic AF accompanied by atrial arrest in their forties [30]. Another mutation, R150Q, has previously been described in six AF families and is characterized by progressive, extreme biatrial dilatation and atrial standstill [31]. ANP is a circulating hormone that, via stimulation of the intracellular second messenger cGMP, plays a primary physiological role in the regulation of intravascular blood volume and vascular tone by means of natriuresis, diuresis, and vasodilatation. Moreover, cGMP signaling triggered by ANP has been shown to shorten both atrial conduction times and the effective refractory period, thus providing an arrhythmia substrate by direct modulation of cardiac ion channel properties [32,33]. However, the electrophysiological effect of these *NPPA* mutations on the cardiomyocytes themselves remains elusive.

4. Genetic basis of conduction block

4.1. LMNA

The *LMNA* gene encodes the ubiquitous inner-nuclear membrane protein lamin A/C, responsible for maintaining the structural integrity and stability of the nuclear envelope. *LMNA* is further involved in various nuclear functions such as gene replication and chromatin organization [34]. Mutations in *LMNA* result in laminopathy, a wide spectrum of phenotypes with at least eleven distinct diseases [34]. Of these, progressive conduction block with DCM is the most frequently described cardiac phenotype [35]. *LMNA*-related DCM leads to severe and progressive damage to the heart, resulting in a higher risk of sudden cardiac death [36]. Male carriers have a worse prognosis due to the high prevalence of malignant ventricular arrhythmias and end-stage heart failure [37,38]. Knock-in mice for H222P-*LMNA* display male predominance for high mortality and progression of heart failure and provide a satisfactory mouse model for laminopathy [39].

4.2. Mutations in sodium channel complex genes

SCN1B mutations have been reported in patients with cardiac conduction abnormalities associated with Brugada syndrome [40]. *SCN1B* encodes the auxiliary Na^+ channel subunit Navβ1 that increases the current density of Nav1.5 [13].

A new gene responsible for cardiac conduction is *SCN10A* that encodes the neuronal Na^+ channel Nav1.8. Several genome-wide association studies (GWAS) have demonstrated that variation of *SCN10A* has a significant impact on resting heart rate, PR duration, and QRS intervals in the general population [41] despite the extremely low level of *SCN10A* expression in the heart. The precise mechanisms underlying *SCN10A* variation modulation of cardiac conduction properties and arrhythmia triggers, such as BrS and AF, are not fully elucidated. A possibility is that mediation could be directed by the activities of the autonomic nervous system, in which *SCN10A* is predominantly expressed [42–44].

4.3. GJA5 (Cx40)

Additional electrical modulators for rapid electrical propagation in the CCS are gap junction channels formed by connexins (Cx) [45]. In the heart, three major Cx subtypes are expressed; namely Cx40, Cx43, and Cx45; that together form a hexameric Cx complex (connexon) at the cell membrane [45]. Gap junction channels are composed of two connexons between two adjacent cardiomyocytes and allow for rapid electrical conduction by passing signal molecules and ions. Of the three Cx subtypes, the high conductance Cx40 is exclusively expressed in the atrium and CCS [45]. A *GJA5* gene mutation, Q58L, has been reported to be associated with progressive familial conduction block and sudden cardiac death [46]. Heterologously expressed mutant Cx40 shows a profound reduction in gap junction conductance, as well as defective formation of membrane plaques. When the structural analysis of Cx26 is compared with Cx40, residue Q58 of Cx40 is expected to form symmetric hydrogen bonds to the same residue of the opposite monomer in parallel [47]. Therefore, Q58L-Cx40 in all likelihood has a structural abnormality that prevents assembly of two Cx40 hexamers.

4.4. KCNJ2

KCNJ2 is the gene responsible for encoding the inward rectifier potassium channel Kir2.1 and is the major regulator of excitability and resting membrane potential in most cardiomyocytes, with the exception of nodal cells [48]. To date, over 40 loss-of-function mutations in *KCNJ2* have been identified in approximately 70% of patients with Andersen–Tawil syndrome, a condition diagnosed using the clinical triad of periodic paralysis, dysmorphic features, and ventricular arrhythmia [49]. However, *KCNJ2* mutation carriers do not always present with the clinical triad [50] and conduction

Please cite this article as: Ishikawa T, et al. Inherited bradyarrhythmia: A diverse genetic background. J Arrhythmia (2015), http://dx.doi.org/10.1016/j.joa.2015.09.009i

abnormalities, such as first-degree AVB and BBB, have been documented in 23% of cases [51].

4.5. TRPM4

TRPM4 encodes the Ca^{2+}-activated transient receptor potential cation channel subfamily M member 4 and is preferentially expressed in Purkinje fibers and the right ventricle [52]. The first responsible loci for progressive familial conduction block was found in 19q13 [53] and was identified as *TRPM4* [54]. Further genetic screening of various conduction disturbances has shown a high prevalence of *TRPM4* mutations in the right BBB (26%; 5 of 19 probands) and AVB (12%; 3 of 26 probands) [55]. Mutations in *TRPM4* have been further identified in cases of Brugada syndrome (4.4%; 11 in 248 probands) [56].

4.6. KCNK17

A mutation in the *KCNK17* gene encoding the pH-sensitive cardiac two-pore domain potassium channel (K2P) TASK-4 has been identified as a contributor to progressive and severe cardiac conduction disorder combined with idiopathic ventricular fibrillation by whole exome sequencing [57]. Mutant TASK-4 channels generated a three-fold increase in currents, while surface expression unchanged. Overexpression of the mutant TASK-4 leads to hyperpolarization and strong inhibition of the upstroke velocity in the spontaneously beating cardiomyocyte cell line HL-1. Strong expression of *KCNK17* has been observed in human Purkinje cells. These results support the likelihood that TASK-4 is functionally relevant for cardiac conduction disorders [57]. However, no specific TASK-4 blockers are available and mice do not functionally express the *KCNK17* gene; thus, little is known regarding the function and role of TASK-4 in the heart.

5. Genes involved in cardiac development and bradycardia

Development of the CCS is a complex biological process with the potential to be wrought with problems. Several transcription factors, including homeodomain proteins and T-box proteins, are essential for CCS morphogenesis and the activation or repression of key regulatory genes [58]. Of the cardiogenic transcription factor genes; *GATA4*, *NKX2-5*, *TBX3*, and *TBX5* play key roles in the development of the primary and second heart fields, while mutation results in congenital heart diseases such as patent foramen ovale, itself often associated with conduction disorders [59]. Holt–Oram syndrome is an inherited, multi-organ anomaly caused by *TBX5* mutation [60]. As *TBX5* promotes the expression of several genes involved in the development of the upper limbs, varying degrees of upper limb abnormalities have been recognized in Holt–Oram syndrome cases. Approximately 75% of probands have cardiac anomalies, whereas about 40% of affected family members present only with ECG abnormalities and without heart malformations [61]. Common ECG abnormalities include first degree AVB and bradycardia [61], which is in line with the preferential expression of *TBX5* in the endocardial cushion region during the developmental stage. The vast majority of *TBX5* mutations in Holt–Oram syndrome are truncation mutations that often delete the T-box domain and result in haplo-insufficiency of T-box activity. In contrast, most missense mutations result in less severe anomalies as the full protein structure is well preserved. A missense mutation, G125R, has been identified in a family suffering from faint digit abnormalities and a higher prevalence of AF without heart malformation [62]. AF is believed to be associated with the increased expression of *NPPA*, *GJA5*, *KCNJ2*, and *TBX3* [62].

6. Advanced genetic and genomic technologies

Many of the causative genes described here were identified using a candidate gene approach, in which genes are selected based on findings of preceding genetic linkage analysis or molecular pathway information [63]. Considering that the human genome encodes at least 20,000 protein-coding genes, the candidate gene approach focuses only on a small fraction of the genome with the remainder unanalyzed. Genome-wide association studies (GWAS) using single nucleotide polymorphisms (SNPs) can significantly expedite linkage analysis by narrowing the regions of interest for further directed sequencing. GWAS has been used in the cardiac electrophysiological field and has resulted in the identification of several new loci involved in long QT syndrome, a key role for calcium signaling pathways in myocardial repolarization [64], and many other ECG parameters [41,65].

GWAS on heart rate revealed the genetic heterogeneity of heart rate regulation and 21 loci were identified; including *HCN4*, gap junction gene *GJA1*, and the atrial α-myosin heavy chain (α-MHC) gene *MYH6* [41]. A rare *MYH6* variant, R721W, that predisposes individuals to SSS susceptibility has been previously identified [66]; however, the disease-causing *MYH6* mutations for familial SSS and their underlying mechanisms remain unknown. We screened nine genotype-negative probands with SSS families for mutations in *MYH6* and identified an in-frame 3-bp deletion that was predicted to delete one residue (delE933) at the highly conserved coiled-coil structure within the binding motif of myosin-binding protein C in one patient [66]. Irregular fluorescent speckles retained in the cytoplasm with substantially disrupted sarcomere striation have been observed in neonatal rat cardiomyocytes transfected with α-MHC mutants carrying delE933 or R721W. In addition to sarcomere impairments, delE933 α-MHC exhibited electrophysiological abnormalities both in vitro and in vivo. The atrial cardiomyocyte cell line HL-1 stably expressing delE933 α-MHC showed a significantly slower conduction velocity on multielectrode array when compared with those of wild-type α-MHC or control plasmid transfected cells. Furthermore, targeted morpholino knockdown of *MYH6* in zebrafish resulted in significantly reduced heart rate that could be rescued by co-expressed wild-type human α-MHC and not by delE933 α-MHC. These data reinforces the relevance of *MYH6* in sinus node function and suggests that structural damage to the sarcomere and functional impairment of atrial action potential propagation may underlie familial SSS with *MYH6* mutations [66].

7. Conclusions

It is now clear that a number of genes are involved in inherited bradyarrhythmia. Recent genetic studies have demonstrated that inherited arrhythmia is attributable to many genes with diverse functions. While the precise underlying mechanisms remain to be elucidated; these genetic defects may disrupt important cardiac functions including electrophysiological properties, development, cardioprotection, and the structural integrity of the membrane and sarcomere, ultimately leading to bradyarrhythmia. However, there are a large number of patients suffering from bradyarrhythmia whose etiologies remain unknown. As we have recently identified a novel *MYH6* mutation based on the most advanced genomic findings using GWAS to investigate SSS [66], new technologies such as next generation sequencing may provide the opportunity to identify new genes for inherited bradyarrhythmia as well as novel insights into the molecular mechanisms behind cardiac rhythm regulation.

Please cite this article as: Ishikawa T, et al. Inherited bradyarrhythmia: A diverse genetic background. J Arrhythmia (2015), http://dx.doi.org/10.1016/j.joa.2015.09.009i

Conflict of interest

The authors have no conflicts of interest to declare.

Acknowledgment

This work was supported by Grants-in-Aid for Scientific Research 26860572 (T.I.), 15H04823 and 15K15311 (N.M.) from the Ministry of Education, Culture, Sports, Science, and Technology of Japan; Health Science Research grants from the Ministry of Health, Labor, and Welfare of Japan for Clinical Research on Measures for Intractable Diseases (H26-002, H26-084, H27-019 and H27-032, N. M.); Translational Research Funds from the Japan Circulation Society (N.M.); the Joint Usage/Research Program of Medical Research Institute, Tokyo Medical and Dental University (N.M.); and a research grant from Takeda Science Foundation (T.I.).

References

[1] Karagueuzian HS. Targeting cardiac fibrosis: a new frontier in antiarrhythmic therapy? Am J Cardiovasc Dis 2011;1:101–9.
[2] Gazoti Debessa CR, Mesiano Maifrino LB, Rodrigues de Souza R. Age related changes of the collagen network of the human heart. Mech Ageing Dev 2001;122:1049–58.
[3] Boyett MR, Honjo H, Kodama I. The sinoatrial node, a heterogeneous pacemaker structure. Cardiovasc Res 2000;47:658–87.
[4] Chandler NJ, Greener ID, Tellez JO, et al. Molecular architecture of the human sinus node: insights into the function of the cardiac pacemaker. Circulation 2009;119:1562–75.
[5] Butters TD, Aslanidi OV, Inada S, et al. Mechanistic links between Na+ channel (SCN5A) mutations and impaired cardiac pacemaking in sick sinus syndrome. Circ Res 2010;107:126–37.
[6] Lakatta EG, Maltsev VA, Vinogradova TM. A coupled SYSTEM of intracellular Ca^{2+} clocks and surface membrane voltage clocks controls the timekeeping mechanism of the heart's pacemaker. Circ Res 2010;106:659–73.
[7] Milano A, Vermeer AM, Lodder EM, et al. HCN4 mutations in multiple families with bradycardia and left ventricular noncompaction cardiomyopathy. J Am Coll Cardiol 2014;64:745–56.
[8] Schulze-Bahr E, Neu A, Friederich P, et al. Pacemaker channel dysfunction in a patient with sinus node disease. J Clin Invest 2003;111:1537–45.
[9] DiFrancesco D. Funny channel gene mutations associated with arrhythmias. J Physiol 2013;591:4117–24.
[10] Verkerk AO, Wilders R. Pacemaker activity of the human sinoatrial node: effects of HCN4 mutations on the hyperpolarization-activated current. Europace 2014;16:384–95.
[11] Xu X, Marni F, Wu S, et al. Local and global interpretations of a disease-causing mutation near the ligand entry path in hyperpolarization-activated cAMP-gated channel. Structure 2012;20:2116–23.
[12] Schweizer PA, Schroter J, Greiner S, et al. The symptom complex of familial sinus node dysfunction and myocardial noncompaction is associated with mutations in the HCN4 channel. J Am Coll Cardiol 2014;64:757–67.
[13] Remme CA. Cardiac sodium channelopathy associated with SCN5A mutations: electrophysiological, molecular and genetic aspects. J Physiol 2013;591:4099–116.
[14] Makita N, Behr E, Shimizu W, et al. The E1784K mutation in SCN5A is associated with mixed clinical phenotype of type 3 long QT syndrome. J Clin Invest 2008;118:2219–29.
[15] Kusano KF, Taniyama M, Nakamura K, et al. Atrial fibrillation in patients with Brugada syndrome relationships of gene mutation, electrophysiology, and clinical backgrounds. J Am Coll Cardiol 2008;51:1169–75.
[16] Abe K, Machida T, Sumitomo N, et al. Sodium channelopathy underlying familial sick sinus syndrome with early onset and predominantly male characteristics. Circ Arrhythm Electrophysiol 2014;7:511–7.
[17] Mohler PJ, Schott JJ, Gramolini AO, et al. Ankyrin-B mutation causes type 4 long-QT cardiac arrhythmia and sudden cardiac death. Nature 2003;421: 634–639.
[18] Mohler PJ, Splawski I, Napolitano C, et al. A cardiac arrhythmia syndrome caused by loss of ankyrin-B function. Proc Natl Acad Sci USA 2004;101: 9137–9142.
[19] Mohler PJ, Davis JQ, Davis LH, et al. Inositol 1,4,5-trisphosphate receptor localization and stability in neonatal cardiomyocytes requires interaction with ankyrin-B. J Biol Chem 2004;279:12980–7.
[20] Mohler PJ, Davis JQ, Bennett V. Ankyrin-B coordinates the Na/K ATPase, Na/Ca exchanger, and InsP3 receptor in a cardiac T-tubule/SR microdomain. PLoS Biol 2005;3:e423.
[21] Koschak A, Reimer D, Huber I, et al. alpha 1D (Cav1.3) subunits can form l-type Ca^{2+} channels activating at negative voltages. J Biol Chem 2001;276:22100–6.
[22] Baig SM, Koschak A, Lieb A, et al. Loss of Ca(v)1.3 (CACNA1D) function in a human channelopathy with bradycardia and congenital deafness. Nat Neurosci 2011;14:77–84.
[23] Christel CJ, Cardona N, Mesirca P, et al. Distinct localization and modulation of Cav1.2 and Cav1.3 L-type Ca^{2+} channels in mouse sinoatrial node. J Physiol 2012;590:6327–42.
[24] Postma AV, Denjoy I, Hoorntje TM, et al. Absence of calsequestrin 2 causes severe forms of catecholaminergic polymorphic ventricular tachycardia. Circ Res 2002;91:e21–6.
[25] Postma AV, Denjoy I, Kamblock J, et al. Catecholaminergic polymorphic ventricular tachycardia: RYR2 mutations, bradycardia, and follow up of the patients. J Med Genet 2005;42:863–70.
[26] Glukhov AV, Kalyanasundaram A, Lou Q, et al. Calsequestrin 2 deletion causes sinoatrial node dysfunction and atrial arrhythmias associated with altered sarcoplasmic reticulum calcium cycling and degenerative fibrosis within the mouse atrial pacemaker complex1. Eur Heart J 2015;36:686–97.
[27] Venetucci L, Denegri M, Napolitano C, et al. Inherited calcium channelopathies in the pathophysiology of arrhythmias. Nat Rev Cardiol 2012;9: 561–575.
[28] Baskar S, Ackerman MJ, Clements D, et al. Compound heterozygous mutations in the SCN5A-encoded Nav1.5 cardiac sodium channel resulting in atrial standstill and His-Purkinje system disease. J Pediatr 2014;165:1050–2.
[29] Chiang DY, Kim JJ, Valdes SO, et al. Loss-of-function SCN5A mutations associated with sinus node dysfunction, atrial arrhythmias, and poor pacemaker capture. Circ Arrhythm Electrophysiol 2015;8(5):1105–12. http://dx.doi.org/10.1161/CIRCEP.115.003098.
[30] Hodgson-Zingman DM, Karst ML, Zingman LV, et al. Atrial natriuretic peptide frameshift mutation in familial atrial fibrillation. N Engl J Med 2008;359: 158–165.
[31] Disertori M, Quintarelli S, Grasso M, et al. Autosomal recessive atrial dilated cardiomyopathy with standstill evolution associated with mutation of natriuretic peptide precursor A. Circ Cardiovasc Genet 2013;6:27–36.
[32] Crozier I, Richards AM, Foy SG, et al. Electrophysiological effects of atrial natriuretic peptide on the cardiac conduction system in man. Pacing Clin Electrophysiol 1993;16:738–42.
[33] Kecskemeti V, Pacher P, Pankucsi C, et al. Comparative study of cardiac electrophysiological effects of atrial natriuretic peptide. Mol Cell Biochem 1996;160–161:53–9.
[34] Capell BC, Collins FS. Human laminopathies: nuclei gone genetically awry. Nat Rev Genet 2006;7:940–52.
[35] Fatkin D, MacRae C, Sasaki T, et al. Missense mutations in the rod domain of the lamin A/C gene as causes of dilated cardiomyopathy and conduction-system disease. N Engl J Med 1999;341:1715–24.
[36] Becane HM, Bonne G, Varnous S, et al. High incidence of sudden death with conduction system and myocardial disease due to lamins A and C gene mutation. Pacing Clin Electrophysiol 2000;23:1661–6.
[37] van Rijsingen IA, Nannenberg EA, Arbustini E, et al. Gender-specific differences in major cardiac events and mortality in lamin A/C mutation carriers. Eur J Heart Fail 2013;15:376–84.
[38] Arimura T, Onoue K, Takahashi-Tanaka Y, et al. Nuclear accumulation of androgen receptor in gender difference of dilated cardiomyopathy due to lamin A/C mutations. Cardiovasc Res 2013;99:382–94.
[39] Arimura T, Helbling-Leclerc A, Massart C, et al. Mouse model carrying H222P-Lmna mutation develops muscular dystrophy and dilated cardiomyopathy similar to human striated muscle laminopathies. Hum Mol Genet 2005;14:155–69.
[40] Watanabe H, Koopmann TT, Le Scouarnec S, et al. Sodium channel beta1 subunit mutations associated with Brugada syndrome and cardiac conduction disease in humans. J Clin Invest 2008;118:2260–8.
[41] Holm H, Gudbjartsson DF, Arnar DO, et al. Several common variants modulate heart rate, PR interval and QRS duration. Nat Genet 2010;42:117–22.
[42] Verkerk AO, Remme CA, Schumacher CA, et al. Functional Nav1.8 channels in intracardiac neurons: the link between SCN10A and cardiac electrophysiology. Circ Res 2012;111:333–43.
[43] Hu D, Barajas-Martinez H, Pfeiffer R, et al. Mutations in SCN10A are responsible for a large fraction of cases of Brugada syndrome. J Am Coll Cardiol 2014;64:66–79.
[44] Le Scouarnec S, Karakachoff M, Gourraud JB, et al. Testing the burden of rare variation in arrhythmia-susceptibility genes provides new insights into molecular diagnosis for Brugada syndrome. Hum Mol Genet 2015;24: 2757–2763.
[45] Virginijus V, Peter Brink R. Biophysical properties of gap junctions. In: Douglas P, Zipes Jose J, editors. Cardiac electrophysiology. 6th ed. Elsevier; 2014. p. 151–60.
[46] Makita N, Seki A, Sumitomo N, et al. A connexin40 mutation associated with a malignant variant of progressive familial heart block type I. Circ Arrhythm Electrophysiol 2012;5:163–72.
[47] Maeda S, Nakagawa S, Suga M, et al. Structure of the connexin 26 gap junction channel at 3.5 A resolution. Nature 2009;458:597–602.
[48] Jeanne Nerbonne M. Voltage-regulated potassium channels. In: Douglas P, Zipes Jose J, editors. Cardiac electrophysiology. 6th ed. Elsevier; 2014. p. 23–32.
[49] Nguyen HL, Pieper GH, Wilders R. Andersen–Tawil syndrome: clinical and molecular aspects. Int J Cardiol 2013;170:1–16.
[50] Kimura H, Zhou J, Kawamura M, et al. Phenotype variability in patients carrying KCNJ2 mutations. Circ Cardiovasc Genet 2012;5:344–53.

Please cite this article as: Ishikawa T, et al. Inherited bradyarrhythmia: A diverse genetic background. J Arrhythmia (2015), http://dx.doi.org/10.1016/j.joa.2015.09.009i

[51] Zhang L, Benson DW, Tristani-Firouzi M, et al. Electrocardiographic features in Andersen–Tawil syndrome patients with KCNJ2 mutations: characteristic T-U-wave patterns predict the KCNJ2 genotype. Circulation 2005;111:2720–6.
[52] Liu H, El Zein L, Kruse M, et al. Gain-of-function mutations in TRPM4 cause autosomal dominant isolated cardiac conduction disease. Circ Cardiovasc Genet 2010;3:374–85.
[53] Brink PA, Ferreira A, Moolman JC, et al. Gene for progressive familial heart block type I maps to chromosome 19q13. Circulation 1995;91:1633–40.
[54] Kruse M, Schulze-Bahr E, Corfield V, et al. Impaired endocytosis of the ion channel TRPM4 is associated with human progressive familial heart block type I. J Clin Invest 2009;119:2737–44.
[55] Stallmeyer B, Zumhagen S, Denjoy I, et al. Mutational spectrum in the Ca(2+)-activated cation channel gene TRPM4 in patients with cardiac conductance disturbances. Hum Mutat 2012;33:109–17.
[56] Liu H, Chatel S, Simard C, et al. Molecular genetics and functional anomalies in a series of 248 Brugada cases with 11 mutations in the TRPM4 channel. PLoS One 2013;8:e54131.
[57] Friedrich C, Rinne S, Zumhagen S, et al. Gain-of-function mutation in TASK-4 channels and severe cardiac conduction disorder. EMBO Mol Med 2014;6:937–51.
[58] Hatcher CJ, Basson CT. Specification of the cardiac conduction system by transcription factors. Circ Res 2009;105:620–30.
[59] Holt M, Oram S. Familial heart disease with skeletal malformations. Br Heart J 1960;22:236–42.
[60] Basson CT, Bachinsky DR, Lin RC, et al. Mutations in human TBX5 [corrected] cause limb and cardiac malformation in Holt–Oram syndrome. Nat Genet 1997;15:30–5.
[61] Newbury-Ecob RA, Leanage R, Raeburn JA, et al. Holt–Oram syndrome: a clinical genetic study. J Med Genet 1996;33:300–7.
[62] Postma AV, van de Meerakker JB, Mathijssen IB, et al. A gain-of-function TBX5 mutation is associated with atypical Holt–Oram syndrome and paroxysmal atrial fibrillation. Circ Res 2008;102:1433–42.
[63] Tabor HK, Risch NJ, Myers RM. Candidate-gene approaches for studying complex genetic traits: practical considerations. Nat Rev Genet 2002;3:391–7.
[64] Arking DE, Pulit SL, Crotti L, et al. Genetic association study of QT interval highlights role for calcium signaling pathways in myocardial repolarization. Nat Genet 2014;46:826–36.
[65] Sotoodehnia N, Isaacs A, de Bakker PI, et al. Common variants in 22 loci are associated with QRS duration and cardiac ventricular conduction. Nat Genet 2010;42:1068–76.
[66] Holm H, Gudbjartsson DF, Sulem P, et al. A rare variant in MYH6 is associated with high risk of sick sinus syndrome. Nat Genet 2011;43:316–20.

Please cite this article as: Ishikawa T, et al. Inherited bradyarrhythmia: A diverse genetic background. J Arrhythmia (2015), http://dx.doi.org/10.1016/j.joa.2015.09.009i

Original Article

Novel Mutation in the α-Myosin Heavy Chain Gene Is Associated With Sick Sinus Syndrome

Taisuke Ishikawa, DVM, PhD; Chuanchau J. Jou, DO, PhD; Akihiko Nogami, MD, PhD; Shinya Kowase, MD; Cammon B. Arrington, MD, PhD; Spencer M. Barnett, BS; Daniel T. Harrell, BS; Takuro Arimura, DVM, PhD; Yukiomi Tsuji, MD, PhD; Akinori Kimura, MD, PhD; Naomasa Makita, MD, PhD

Background—Recent genome-wide association studies have demonstrated an association between *MYH6*, the gene encoding α-myosin heavy chain (α-MHC), and sinus node function in the general population. Moreover, a rare *MYH6* variant, R721W, predisposing susceptibility to sick sinus syndrome has been identified. However, the existence of disease-causing *MYH6* mutations for familial sick sinus syndrome and their underlying mechanisms remain unknown.

Methods and Results—We screened 9 genotype-negative probands with sick sinus syndrome families for mutations in *MYH6* and identified an in-frame 3-bp deletion predicted to delete one residue (delE933) at the highly conserved coiled-coil structure within the binding motif to myosin-binding protein C in one patient. Co-immunoprecipitation analysis revealed enhanced binding of delE933 α-MHC to myosin-binding protein C. Irregular fluorescent speckles retained in the cytoplasm with substantially disrupted sarcomere striation were observed in neonatal rat cardiomyocytes transfected with α-MHC mutants carrying delE933 or R721W. In addition to the sarcomere impairments, delE933 α-MHC exhibited electrophysiological abnormalities both in vitro and in vivo. The atrial cardiomyocyte cell line HL-1 stably expressing delE933 α-MHC showed a significantly slower conduction velocity on multielectrode array than those of wild-type α-MHC or control plasmid transfected cells. Furthermore, targeted morpholino knockdown of *MYH6* in zebrafish significantly reduced the heart rate, which was rescued by coexpressed wild-type human α-MHC but not by delE933 α-MHC.

Conclusions—The novel *MYH6* mutation delE933 causes both structural damage of the sarcomere and functional impairments on atrial action propagation. This report reinforces the relevance of *MYH6* for sinus node function and identifies a novel pathophysiology underlying familial sick sinus syndrome. (***Circ Arrhythm Electrophysiol.* 2015;8:400-408. DOI: 10.1161/CIRCEP.114.002534.**)

Key words: genetics ■ MYH6 ■ myosin heavy chain ■ sick sinus syndrome ■ sinus node dysfunction

Sick sinus syndrome (SSS) is a common arrhythmia often associated with aging, structural heart diseases, or surgical injury, but can also occur in a familial form.[1] Several studies have demonstrated genetic mutations in both sporadic and familial cases of SSS.[2–4] Affected ion channel or ion channel–associated genes identified to date include sodium channel, Nav1.5 (*SCN5A*),[2] ankyrin-B (*ANK2*),[3] and hyperpolarization-activated channel (*HCN4*).[4] Mutations in *HCN4* result in sinus node dysfunction caused by a reduction of the pacemaker current, whereas *SCN5A* mutations lead to conduction delay within the sinus node or exit block.[5]

MYH6 and *MYH7* encode the homologous myosin heavy chain (MHC) isoforms α-MHC and β-MHC, respectively, in cardiomyocytes, which play pivotal roles in the organization of sarcomeric structures and muscle contraction.[6–8] *MYH7* is predominantly expressed in the adult ventricle, whereas *MYH6* is mainly expressed in the fetal heart and adult atrium.[9] *MYH7* is a well-established causative gene with over 300 mutations responsible for hypertrophic cardiomyopathy and dilated cardiomyopathy,[10,11] whereas more limited *MYH6* mutations have been reported in cardiomyopathy[12,13] and congenital heart disease, such as atrial septal defect.[7,14–17] On the contrary, recent genome-wide association studies demonstrated that a common nonsynonymous variant A1101V in *MYH6* was associated with an increased resting heart rate,[17–19] whereas another rare nonsynonymous variant (resulting in R721W) was associated with a high risk of SSS.[20]

Received November 12, 2014; accepted February 11, 2015.

From the Department of Molecular Physiology, Nagasaki University Graduate School of Biomedical Sciences, Nagasaki (T.I., D.T.H., Y.T., N.M.); Department of Molecular Pathogenesis, Medical Research Institute, Tokyo Medical and Dental University, Tokyo, Japan (T.I., T.A., A.K.); Division of Pediatric Cardiology, University of Utah, Salt Lake City (C.J.J., C.B.A., S.M.B.); Cardiovascular Division, University of Tsukuba, Tsukuba (A.N.); Department of Heart Rhythm Management, Yokohama Rosai Hospital, Yokohama (A.N., S.K.); and Department of Veterinary Medicine, Kagoshima University, Kagoshima, Japan (T.A.).

The Data Supplement is available at http://circep.ahajournals.org/lookup/suppl/doi:10.1161/CIRCEP.114.002534/-/DC1.

Correspondence to Naomasa Makita, MD, PhD, Department of Molecular Physiology, Nagasaki University, Graduate School of Biomedical Sciences, 1-12-4 Sakamoto, Nagasaki 852–8523, Japan, E-mail makitan@nagasaki-u.ac.jp or Akinori Kimura, MD, PhD, Department of Molecular Pathogenesis, Medical Research Institute, Tokyo Medical and Dental University, 1-5-45 Yushima, Bunkyo-ku, Tokyo 113–8510, Japan, E-mail akitis@mri.tmd.ac.jp

Circ Arrhythm Electrophysiol **is available at http://circep.ahajournals.org** **DOI: 10.1161/CIRCEP.114.002534**

WHAT IS KNOWN

- Sick sinus syndrome (SSS) is often associated with aging and structural heart diseases, but it may occur in a familial form.
- Recent genome-wide association studies uncovered MYH6 encoding atrial myosin heavy chain as a susceptibility gene for heart rate and SSS; however, its underlying mechanisms and the existence of causative mutations for SSS remain unknown.
- Here, we report a novel *MYH6* mutation delE933 in an SSS patient who has a family history of SSS.

WHAT THE STUDY ADDS

- When expressed in cardiomyocytes, delE933-*MYH6* impaired the atrial action potential propagation and disrupted sarcomere integrity consistent with the R721W-*MYH6*, a high risk genetic predisposition for SSS demonstrated in Icelanders.
- Our data reinforces the relevance of *MYH6* of sinus node function and suggested that structural damages of the sarcomere and functional impairments on atrial action potential propagation may underlie familial SSS with *MYH6* mutations.

Moreover, heterozygous zebrafish carrying the *MYH6* mutation N695K (*MYH6*$^{tm423/+}$) displayed partial atrial contractile defects.[21] Based on these observations, it is conceivable that some *MYH6* variations impair the sarcomere structure and function of the atrium, which in turn would cause electrophysiological abnormalities and sinus node dysfunction. However, it remains to be elucidated whether (1) *MYH6* is the causative gene for familial SSS and (2) the genetic variations of *MYH6* associated with SSS confer pacemaker dysfunction through structural damage of the sarcomere of the atrial muscle surrounding the sinus node or by functional impairment of the pacemaker channel or sodium channel. The present study identified a novel *MYH6* mutation in one SSS proband and investigated the means by which this could confer sinus node dysfunction.

Methods

Genetic Screening of *MYH6* Mutations

We previously performed genetic screening of mutations in *SCN5A* and *HCN4* in 15 probands afflicted with familial SSS and found 6 distinct *SCN5A* mutations.[22] In this study, we enrolled 9 SSS families out of this cohort, which were free from *SCN5A* or *HCN4* mutations. Age at diagnosis of the probands (3 male and 6 female) ranged from 3 to 65 years old (44.6±21.8 years old; mean±SD).

Genomic DNA was extracted from peripheral blood of each subject using standard methods. Coding regions of *MYH6* were amplified by polymerase chain reaction using exon-flanking intronic primers (Table I in the Data Supplement). Direct DNA sequencing was performed using ABI 3130 genetic analyzers (Life Technologies, Carlsbad, CA). Mutations were validated by the analysis of unrelated 400 healthy Japanese individuals and dbSNP, 1000 Genome Project, Exome Variant Server, and Human Genetic Variation Database (HGVD, Japanese variation database, http://www.genome.med.kyoto-u.ac.jp/SnpDB/). All probands and family members who participated in the study gave their written informed consent in accordance with the Declaration of Helsinki. The research protocol was approved by the Ethics Review Committee of Nagasaki University and the Ethics Review Committee of Medical Research Institute, Tokyo Medical and Dental University.

Alignment of Amino Acid Sequences and Structural Prediction of α-MHC

Amino acid sequence of human α-MHC was aligned using the HomoloGene program with those of other species, and the phylogenetic conservations were testified among human MHC isoforms (the GenBank accession number of each gene is listed in Tables II and III in the Data Supplement). Alterations of the coiled-coil structure of the α-MHC were predicted in silico by using SWISS-MODEL (http://swissmodel.expasy.org/) and visualized by a software RasTop (http://www.geneinfinity.org/rastop/).

Plasmids and cRNA preparation

A 5.8 kb cDNA fragment of human *MYH6* was obtained by reverse transcription-polymerase chain reaction from human heart RNA using a primer pair *MYH6*-F-EcoRV and *MYH6*-R-SalI (Table I in the Data Supplement) and was cloned into pEGFP-C1 (Takara Bio, Shiga, Japan) to make green fluorescent protein (GFP)-tagged *MYH6* plasmid (pEGFP-*MYH6*). Mutant *MYH6* plasmids of R721W (c.2161C>T) and delE933 (c.2797_2799delGAG) were constructed using an overlap-extension polymerase chain reaction strategy.

To assess the binding affinity of the mutant S2 region of α-MHC to myosin-binding protein C (MyBP-C) on the basis of the previous report,[8] cDNAs corresponding to the binding regions for human α-MHC (S2 region; aa. 884–965 of NP_002462) and human MyBP-C (C1C2 region; aa. 256–363 of NP_000247) were amplified and cloned into the c-myc-tag plasmid pCMV-Tag3B (Takara Bio; pCMV3B-*MYH6*-S2) and the pEGFP-C1 (pEGFP-*MYBPC3*-C1C2), respectively. All constructs were sequenced to ensure that no errors were introduced.

For the zebrafish experiments, wild-type (WT) and mutant *MYH6* cDNA fragments were, respectively, cloned into pIRES2-EGFP vector (Takara Bio; pIRES2-EGFP-*MYH6*) and pCS2+ vector[23] (pCS2-*MYH6*) by using specific primer pairs (Table I in the Data Supplement). cRNAs of human *MYH6* were synthesized using the mMessage mMachine in vitro transcription kit (Life Technologies) and purified as described previously.[24] Purified mutant cRNAs were sequenced by the University of Utah sequencing core facility.

Coimmunoprecipitation Assay

HeLa cells were cotransfected with pEGFP-*MYBPC3*-C1C2 and pCMV3B-*MYH6*-S2 using Transfectin lipid reagent (BioRad, Hercules, CA). After 48 hours of the transfection, cells were lysed in protein extraction buffer (1% Nonidet P-40, 1 mmol/L EDTA, 150 mmol/L NaCl, and 10 mmol/L Tris-HCl, pH 7.8) containing Protease Inhibitor Cocktail. Total cellular lysate was obtained by centrifugation at 13000*g* for 5 minutes, and its protein concentration was measured by BCA (bicinchoninic acid) protein assay (Thermo Fisher Scientific, Waltham, MA). Coimmunoprecipitation assay was performed using equal amount of cellular lysate with goat anti-myc polyclonal antibody (Sigma-Aldrich, St. Louis, MO) using the Catch and Release version 2.0 reversible immunoprecipitation system (Millipore, Billerica, MA). Immunoprecipitates were separated on a 9% SDS-polyacrylamide gel and transferred to a nitrocellulose membrane. After blocking with 5% skim milk in PBS, membranes were incubated with primary anti-GFP monoclonal antibody (1:100, Santa Cruz Biotechnology, Dallas, TX) overnight at 4°C and rabbit-anti mouse IgG horseradish peroxidase (HRP)–conjugated antibody (Dako, Grostrup, Denmark) for 1 hour at RT. Signals were visualized by Immobilon Western Chemiluminescent HRP Substrate (Millipore) and Luminescent Image Analyzer LAS-3000 mini (Fujifilm, Tokyo, Japan).

Immunofluorescence Study

Immunohistological study was performed using neonatal rat ventricular cardiomyocytes prepared from 1-day-old Sprague–Dawley rats as described previously.[25] Briefly, neonatal rat ventricular cardiomyocytes (4×10^4) were transfected with WT or mutant pEGFP-*MYH6* plasmid with Lipofectamine LTX. Twenty-four hours later, the cells were fixed with 100% ethanol, stained by primary mouse anti-α-actinin antibody (1:100, Sigma-Aldrich) overnight at 4°C and visualized with secondary Alexa Fluor 568 goat antimouse IgG antibody (1:500, Life Technologies). The fluorescent images were analyzed using LSM510 laser-scanning confocal microscope with a 63× oil immersion objective lens (Carl-Zeiss Microscopy, Jena, Germany).

All care and treatment of animals were in accordance with the guidelines for the Care and Use of Laboratory Animals published by the National Institute of Health (NIH Publication, eighth edition 2011) and subjected to prior approval by the animal protection authorities of Nagasaki University and Tokyo Medical and Dental University.

Action Potential Propagation Velocity Measurements in HL-1 Cells Stably Expressing Human *MYH6*

The mouse atrial cardiomyocyte cell line HL-1 (4×10^5), gift from Dr Claycomb, was cultured as previously described.[26] Cells were transfected with 2 μg of linearized pIRES2-EGFP-*MYH6* plasmids of WT or delE933 or pIRES2-EGFP plasmid and 4 μl of Lipofectamine LTX (Life Technologies) according to the manufacturer's instructions. Forty-eight hours after transfection, cells were cultured in the presence of 400 μg/mL G418 (Life Technologies) for 4 weeks to establish stable cell lines.

Stable HL-1 cells (1×10^5 cells) expressing WT-*MYH6*, delE933-*MYH6*, or mock pIRES2-EGFP were plated on 8×8 planner multi-electrode arrays (array size 1 mm×1 mm; electrode diameter 50 μm; Alpha MED Scientific Inc., Osaka, Japan) precoated with gelatin and fibronectin (Sigma-Aldrich). Seventy-two hours later, a single stimulus of 10 μA was applied on a designated point to initiate spontaneous beating, and electric field potentials were recorded for 1 minute. Action potential propagation velocity was calculated by averaging the velocities between the stimulation point and the remaining 63 points. Cell numbers on the array were counted after recordings with detaching them from the arrays with Trypsin-EDTA. These procedures were repeated 4 times for each line.

In Vivo Evaluation of Overexpressed *MYH6* in Zebrafish

Transgenic zebrafish (cmlc2:GFP, *Danio rerio*) embryos were used to functionally characterize the zebrafish *myh6* and human *MYH6* variant. *MYH6* ATG-blocking morpholino antisense oligonucleotide (myh6 ATG-MO) was designed to target *myh6* (Table I in the Data Supplement).[27] Myh6 ATG-MO (0.5–1 ng/embryo) was injected alone or coinjected with WT or delE933 *MYH6* cRNA (0.4 ng/embryo) at the 1- to 2-cell stage. After the injection, embryos were maintained in embryo water at 28°C and staged according to age and morphological criteria.[28] Cardiac phenotypes were screened using

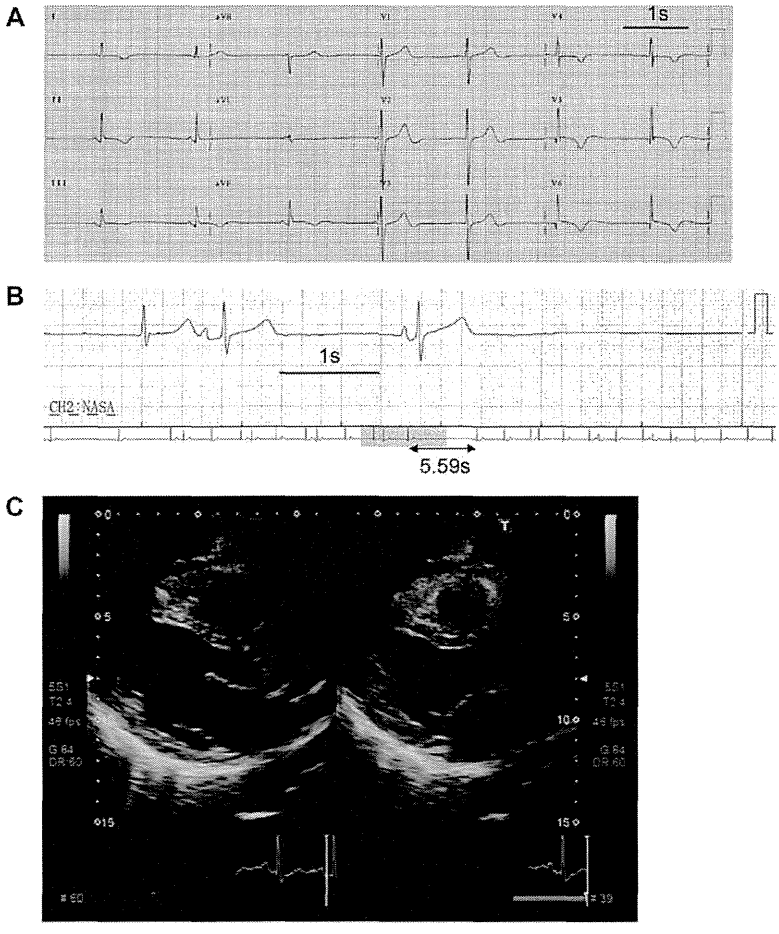

Figure 1. ECG and echocardiography of the sick sinus syndrome (SSS) proband. **A**, ECG recordings of the proband (age 62 years) displayed sinus bradycardia (42 beats per minute) with unusual P wave axis and junctional escape beat (last beat in V4-V6). T waves in I-III, aVF, and V4-6 were inverted. **B**, Holter ECG showed sinus arrest with a maxium RR interval of 5.59 s. **C**, Echocardiography revealed mild dilatation of left ventricle (LV) and right atrium without obvious evidence for cardiomyopathy, congenital heart disease, or cardiac dysfunction. LV internal diameter, 57 mm; LV posterior and interventricular wall thickness, each 6 mm; LV ejection fraction, 63%.

fluorescent microscopy at 48 hour-post-fertilization (hpf). Heart rate and rhythm were recorded. Videos obtained from the embryos were analyzed using Image J (National Institutes of Health) to determine the heart rate and the duration of cardiac pauses.

Statistical Analyses

Results are presented as means±SE otherwise stated, and statistical comparisons were made by using 1-way analysis of variance followed by Bonferroni adjustment to estimate the significance of differences between the mean values of all pairwise. Statistical significance was assumed for $P<0.05$.

Results

Case Presentation

Genetic screening of *MYH6* mutations in 9 probands with familial SSS identified a novel mutation in a 62-year-old Japanese woman. She attended the hospital because of several episodes of presyncope with which she had been afflicted for 5 years. Her 12-lead ECG showed sinus bradycardia (heart rate 42 beats per minute) with unusual P wave axis and junctional escape beat (Figure 1A), and Holter ECG revealed sinus arrest with maximum RR interval of 5.59 s (Figure 1B). She had no history of other arrhythmias, including atrial fibrillation. Echocardiography revealed mild dilatation of the left ventricle (LV) and right atrium, but there were no obvious signs of cardiomyopathy, congenital heart disease, or cardiac dysfunction (LV internal diameter in diastole, 57 mm; LV posterior wall in diastole, 6 mm; interventricular septal wall in diastole, 6 mm; and LV ejection fraction, 63%; Figure 1C). A pacemaker was implanted after the diagnosis of SSS. Her deceased mother also had a pacemaker implanted because of SSS during the 7th decade of her life.

Identification of the Novel *MYH6* Mutation delE933

The novel mutation identified in the proband was an in-frame 3-bp deletion, c.2797_2799delGAG, located in exon 22 of *MYH6*. This was predicted to delete one residue within the glutamic acid triplet at aa.931–933 of α-MHC (delE933; Figure 2A). This triplet is located in the S2 segment of α-MHC, a crucial structure required for binding to MyBP-C and for regional phosphorylation of MyBP-C,[6] thereby facilitating a flexible link between thin and thick filaments. The S2 hinge region is highly conserved among α-MHC from different species, as well as between other MHC isoforms (Figure 2B).

The proband has no siblings or offspring, and DNA was not available from her deceased mother. The delE933 mutation was not identified in 800 *MYH6* alleles from healthy Japanese controls or in the public genetic variation databases of dbSNP, 1000 Genomes, Exome Variant Server, and HGVD. The common variation A1101V was not found in the proband, whereas 3 out of 8 other probands in our cohort were heterozygous for A1101V. The rare *MYH6* variation R721W (c.C2161T), associated with SSS in Icelanders,[20] was not found in our familial SSS cohort. No other disease-related mutations were identified in *SCN5A*, *HCN4*, *SCN3B*, *KCNJ3*, *KCNJ5*, or *GJA5* in our familial SSS cohort. Polymorphisms identified in *MYH6* are listed in Table IV in the Data Supplement.

delE933-*MYH6* Mutation Disrupts Sarcomere Structures

The S2 segment is a coiled-coil domain of α-MHC composed of a motif of heptad repeats of amino acids.[6,29,30] SWISS-MODEL simulation predicted that the delE933 mutation would cause local disruption of the coiled-coil structure (Figure 3A). Immunoprecipitation studies using a recombinant MyBP-C C1-C2 protein and WT and delE933α-MHC S2 region proteins expressed in HeLa cells showed that the binding ability of α-MHC with MyBP-C was substantially enhanced by the delE933 mutation (Figure 3B).

Because structural damage of sarcomere have been reported in association with *MYH6* mutations responsible for atrial

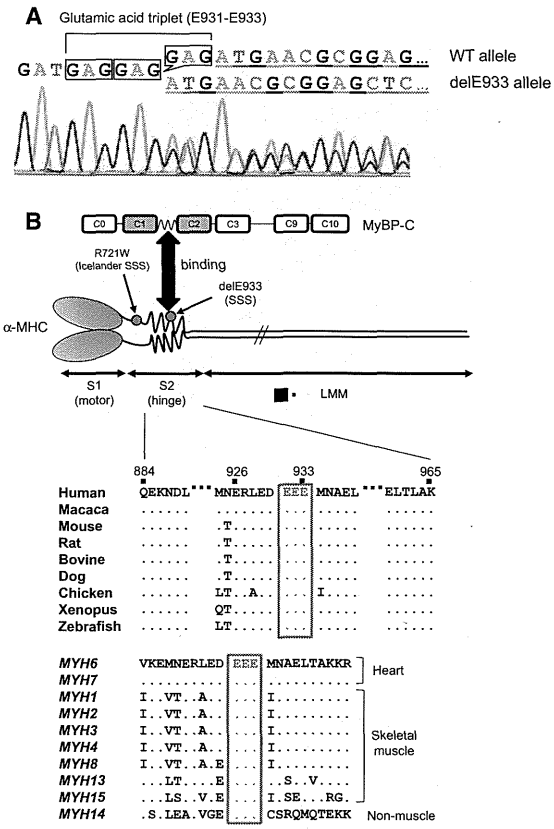

Figure 2. Genetic and protein information of the *MYH6* mutations. **A**, An electropherogram of exon 22 of *MYH6* of the proband. Boxes indicate the codons of triplicate glutamic acids E931-E933 of the wild-type (WT) allele and an in-frame deletion of GAG resulting in delE933. **B**, Protein structures of α-myosin heavy chain (α-MHC) and its binding partner myosin-binding protein C (MyBP-C). α-MHC consists of S1 motor, S2 hinge, and light meromyosin (LMM) regions. The S2 hinge region interacts with the region of MyBP-C between the 1st (C1) and 2nd globular structure (C2). Locations of the 2 *MYH6* mutations, a rare variant R721W identified in Icelanders[20] and delE933 (this study), are shown with red dots. Protein sequence alignment shows that the MyBP-C binding site (residues 884–965) are highly conserved among α-MHCs from different species, and the glutamic acid triplet is perfectly conserved among different species and different MHC isoforms of cardiac (*MYH6*, *MYH7*), skeletal muscle (*MYH1*, *MYH2*, *MYH3*, *MYH4*, *MYH8*, *MYH13*, *MYH15*), and a nonmuscle type (*MYH14*). SSS indicates sick sinus syndrome.

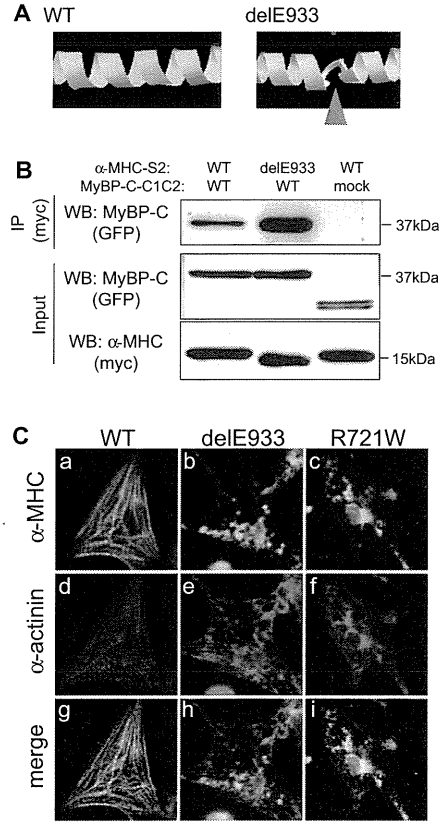

Figure 3. In silico prediction and in vitro functional evaluation of delE933-*MYH6*. **A**, Ribbon representation of 3-dimensional structure of the S2 region in human α-myosin heavy chain (α-MHC) predicted and visualized by SWISS-MODEL and RasTop, respectively. The coiled-coil structure is partially disrupted at the truncated amino acid E933 (arrowhead). **B**, Co-immunoprecipitation study of the S2 region of α-MHC and C1C2 region of cardiac myosin-binding protein C (MyBP-C). The S2 fragment of delE933 shows increased binding to the C1C2 fragment of MyBP-C. A nonspecific double band was often observed on the input of a mock pEGFP-C1 plasmid (third column). **C**, Fluorescence images of neonatal rat ventricular cardiomyocytes transiently expressing wild-type (WT), delE933, or R721W *MYH6* fused to green fluorescent protein (GFP). WT α-MHC shows a striated pattern of GFP together with the proper striated sarcomeric pattern of α-actinin (**a** and **d**). α-MHC with mutations of R721W and delE933 show brightly fluorescent speckles without well-organized sarcomere structure (**b** and **c**). The α-actinin images show a misaligned and disrupted pattern of myofibrils (**e** and **f**), indicating sarcomere disintegration. Scale bar, 10 μm.

septal defect,[7] we next explored whether the *MYH6* variation R721W, as well as delE933, disrupted integrity of sarcomere structures. To investigate the functional consequences of *MYH6* mutations on the atrial sarcomere structure, we used a heterologous expression system in cultured rat cardiomyocytes in which the predominant ventricle MHC isoform is α-MHC.[31] Neonatal rat ventricular cardiomyocytes were transiently transfected with a GFP-tagged *MYH6* WT, delE933, or R721W plasmids. Confocal microscopy analysis revealed comparable GFP intensities after transfection of all 3 *MYH6* plasmids (Figure 3C, a–c), indicating that the expression levels and stability of heterologously expressed α-MHC proteins were similar. Endogenous sarcomeric α-actinin expression at the Z-disc indicated the sarcomere integrity of transfected myocardial cells (Figure 3C, d–f). Cells expressing WT-*MYH6* displayed a striated staining pattern, indicating that heterologous α-MHC was correctly integrated into the sarcomere. However, both *MYH6* mutants, delE933 and R721W, exhibited a substantially disrupted α-actinin staining pattern and perinuclear aggregation of α-MHC, suggesting that structural damage to the sarcomere had occurred in cells expressing *MYH6* variants predisposing to sinus node dysfunction.

Atrial HL-1 Cells Stably Expressing the delE933-*MYH6* Showed Impaired Electric Propagation

A recent genome-wide association study showed that the Iceland-specific *MYH6* variant was significantly associated with atrial fibrillation,[20] we hypothesized that the functional defects caused by mutated *MYH6* may affect action potential propagation in the atrium surrounding the sinus node, leading to SSS manifestation. We cultured the mouse atrial cardiomyocyte cell line HL-1 stably expressing WT or mutant *MYH6* on 64-well electrode arrays and analyzed electric propagation velocities (Figure 4A). The propagation velocity was unchanged between WT-*MYH6* and control mock-transfected cells, but cells expressing delE933-*MYH6* exhibited a significantly slower propagation velocity (control, 3.6±0.6 mm/s; WT, 3.8±1.2 mm/s; delE933, 2.9±0.8 mm/s; n=252 for each line, $P<0.001$ for WT versus delE933; Figure 4B). Cell numbers of each array were comparable ($P=0.49$; Table V in the Data Supplement). These data suggest that mutant *MYH6* delE933 impairs cell-to-cell action potential propagation in the atrial myocardium.

delE933-*MYH6* Failed to Rescue the Heart Rate Reduction in Zebrafish With Morpholino *myh6* Knockdown

To determine whether the human *MYH6* orthologue *myh6* could influence heart rate control in zebrafish, we performed targeted *myh6* knockdown experiments with ATG-MO. Zebrafish cardiac phenotypes, including heart rate and cardiac rhythm, were assessed at 48 hpf. The *myh6* morphants exhibited atrial dilatation (Figure 4C), which is consistent with a previous report using decreased functional *myh6* transcript.[27] *Myh6* morphants also showed a significantly slower heart rate than uninjected embryos (*myh6*-MO, 137.7±2.2 beats per minute, n=28; uninjected 150.2±1.6 beats per minute, n=25; $P<0.001$; Figure 4D). Cardiac asystole was not observed in uninjected embryos or morphants. As shown in Figure 4D, coinjection of WT human *MYH6* cRNA rescued the bradycardia (148.7±1.4 beats per minute, n=26; versus *myh6*-MO $P<0.001$), suggesting that the human *MYH6* compensated for the loss of the zebrafish orthologue. By contrast, human *MYH6* carrying the delE933 mutation failed to rescue the bradycardia (142.3±2.5 beats per minute, n=24). Human *MYH6* RNA was detected by reverse transcription-polymerase chain reaction in embryos at 24 and 48 hours after injection (Figure in the Data Supplement), suggesting that the delE933 mutation of *MYH6* is responsible for sinus node dysfunction.